Single-Carrier SM-MIMO: A Promising Design for Broadband Large-Scale Antenna Systems

Ping Yang, Yue Xiao, Yong Liang Guan, K. Hari, A. Chockalingam, Shinya Sugiura, Harald Haas, Marco Di Renzo, Christos Masouros, Zilong Liu, et al.

Single-Carrier SM-MIMO: A Promising Design for Broadband Large-Scale Antenna Systems

Ping Yang, Yue Xiao, Yong Liang Guan, *Member, IEEE*, K. V. S. Hari, *Fellow, IEEE*, A. Chockalingam, *Senior member, IEEE*, Shinya Sugiura, *Senior member, IEEE*, Harald Haas, *Member, IEEE*, Marco Di Renzo, *Senior member, IEEE*, Christos Masouros, *Senior member, IEEE*, Zilong Liu, Lixia Xiao, Shaoqian Li, *Fellow, IEEE*, and Lajos Hanzo, *Fellow, IEEE*

***Abstract*—The main limitations of employing large-scale antenna (LSA) architectures for broadband frequency-selective channels include, but are not limited to their complexity, power consumption and the high cost of multiple radio frequency (RF) chains. Promising solutions can be found in the recently proposed family of single-carrier (SC) spatial modulation (SM) transmission techniques. Since the SM scheme's transmit antenna (TA) activation process is carried out in the context of a SC-SM architecture, the benefits of a low-complexity and low-cost single-RF transmitter are maintained, while a high MIMO multiplexing gain can be attained. Moreover, owing to its inherent SC structure, the transmit signals of SC-SM have attractive peak power characteristics and a high robustness to RF hardware impairments, such as the RF carrier frequency offset (CFO) and phase noise. In this paper, we present a comprehensive overview of the latest research achievements of SC-SM, which has recently attracted considerable attention. We outline the associated transceiver design, the benefits and potential tradeoffs, the LSA aided multiuser (MU) transmission developments, the relevant open research issues as well as the potential solutions of this appealing transmission technique.**

***Index Terms*—Energy Efficiency, frequency selective channels, large-scale MIMO systems, spatial modulation, single-carrier transmission, single-RF chain, multiuser communication.**

P. Yang, Y. Xiao, L. Xiao and S. Li are with the National Key Laboratory of Science and Technology on Communications, University of Electronic Science and Technology of China 611731, Sichuan, China. (e-mail: yplxw@163.com, xiaoyue@uestc.edu.cn, xiaolixia_cool@163.com, lsq@uestc.edu.cn).

K. V. S. Hari and A. Chockalingam are with the Department of ECE, Indian Institute of Science, India (e-mail: hari, achockal@ece.iisc.ernet.in).

Harald Haas is with the Institute for Digital Communications and the Joint Research Institute for signal and Image Processing, School of Engineering, The University of Edinburgh, U. K. (e-mail: h.haas@ed.ac.uk).

Marco Di Renzo is with the Laboratory of Signals and Systems (L2S), French National Center for Scientific Research (CNRS), University of Paris-Sud XI, 3 rue Joliot-Curie, 91192 Gif-sur-Yvette, France(e-mail: marco.direnzo@lss.supelec.fr).

Y. Guan and Z. Liu are with the School of Electrical and Electronic Engineering, Nanyang Technological University, Singapore (e-mail: EYLGuan,zilongliu@ntu.edu.sg).

S. Sugiura is with the Department of Computer and Information Sciences, Tokyo University of Agriculture and Technology, Koganei, Tokyo 184-8588, Japan (e-mail: sugiura@ieee.org).

Christos Masouros is with the Communications and Information Systems research group, Dept. Electrical & Electronic Engineering, University College London (e-mail: c.masouros@ucl.ac.uk).

L. Hanzo is with the School of Electronics and Computer Science, University of Southampton, Southampton SO17 1BJ, U.K. (e-mail:lh@ecs.soton.ac.uk).

The financial support of the National Science Foundation of China under Grant number 61501095, of the National High-Tech R&D Program of China ("863" Project under Grant number 2014AA01A707), of the European Research Council's Advanced Fellow Grant, of the Royal Academy of Engineering, UK and the Engineering and Physical Sciences Research Council (EPSRC) project EP/M014150/1, and of the National Science Foundation of China under Grant number 60902026 and 61032002, and of the Japan Society for the Promotion of Science (JSPS) KAKENHI Grant Number 26709028 are gratefully acknowledged.

I. Introduction

MULTIPLE-input multiple-output (MIMO) techniques have been widely studied during the last two decades and have been incorporated into most of the recent communication standards [1], [2] due to their benefits of providing diversity, and/or multiplexing gains [3]–[5]. However, in order to satisfy the ever-growing demands for higher capacity, larger coverage area and better reliability, further improved MIMO transceivers should be designed [6].

Pursuing this research objective, the concept of large-scale MIMO (LS-MIMO) techniques has been proposed [6]–[12], which employs tens to hundreds of transmit/receive antennas for dramatically improving the attainable link reliability, spectral efficiency and cellular coverage. Usually, the multiple-antenna front-end architecture requires a separate radio frequency (RF) chain. This means that the cost of MIMO transmitters to scale linearly with the number of antennas [13]. Moreover, the presence of hundreds of antennas will increase the complexity of both the transmit signal generation and detection. Furthermore, the RF power amplifiers and the associated high-dimensional signal processing may erode the energy efficiency of systems, which are responsible for about 55-85% of the total power consumption [14], [15]. These factors exacerbate the practical realization of LS-MIMO systems.

The emerging SM design paradigm constitutes an attractive low-complexity yet energy-efficiency option for the family of LS-MIMO systems, due to its low-cost single-RF-based transmitter, as well as owing to its low-complexity single-stream based detector and its ability to maintain the potential benefits of multiple antennas [16]–[19]. The roots of the SM design philosophy can be traced back

to the combination-based frequency hopping code division multiple access technique (FH-CDMA) proposed in 1980 [20]–[22], where the combination pattern of the frequency bins was used for conveying information, hence resulting in an improved throughput. The first conference paper on single-RF based SM was published in 2006 [23], but its extensive research was mainly fueled by the pioneering works of Haas *et al.* [16]–[18], Mesleh *et al.* [16], [24], [25], followed by Yang *et al.* [26], Sugiura *et al.* [27], Renzo *et al.* [28]–[32], Panayırcı and Poor *et al.* [33], Başar [34], Chang *et al.* [35], [36] as well as Jeganathan *et al.* [37]. Throughout its decade-long history, the SM concept has been termed in different ways and it was extended to different scenarios. The wide-ranging studies disseminated in [23]–[42] have characterized some of the fundamental properties of SM. For example, the attainable bit error rate (BER) performance in different fading channels [23], [29]–[32], [37]–[39], the issues of achieving transmit diversity [27], [28], [31], [40], the effects of channel estimation errors [32], [41], [42], as well as the effects of power imbalance [43] have been characterized. Moreover, some simplified and generalized SM schemes have also been proposed by exploiting the different degrees of freedom offered by the temporal domain, frequency domain and spatial domain fading [17]–[19], [27], such as the space shift keying (SSK), the generalized SSK (GSSK), the generalized SM (GSM), the space-time shift keying (STSK), the space-frequency shift keying (SFSK) and the space-time-frequency shift keying (STFSK) arrangements. It was found that SM and its variants are capable of striking a flexible trade-off amongst the computational complexity imposed, the number of RF chains required, the attainable BER and the achievable transmission rate.

To be specific, SM relies on the unique encoding philosophy of activating one out of numerous transmit antennas (TAs) during each channel-use [23]–[31]. The activated TA then transmits classic complex-valued symbols of amplitude and phase modulation (APM). Since in SM only a single TA is activated at any time instant, its transmitted signal is sparse in the spatial domain. The advantages of SM-MIMO include its low-dimensional signal representation as well as reduced RF hardware complexity, cost, and size [18], [19]. Moreover, it is capable of relaxing the requirement of inter-antenna synchronization and of mitigating the inter-antenna interference of conventional MIMO schemes. Apart from the earlier variants and extensions of SM disseminated in [17]–[19], recently a variety of SM-related classes have been proposed, including those designed for spectrum sharing environments [44], for multiple access transmissions [45], for energy-efficient applications [46], for cooperative SM scenarios [47]–[53] and for closed-loop designs [54]. The above-mentioned potential benefits of SM over the conventional MIMO techniques have been validated not only via numerical simulations [16], [23], [29]–[32], [37]–[39] but also by laboratory experiments [55]–[57].

Despite of its rich literature [23]–[37], the family of SM-related schemes has been predominantly investigated in the context of flat fading channels. In the case of wide-band frequency-selective channels, orthogonal frequency-division multiplexing (OFDM) [58] is generally assumed in SM-related schemes. In this case, multiple TAs have to be simultaneously activated over the OFDM frame, which will jeopardize most of the single-RF benefits of SM-MIMO. Moreover, the OFDM signal has a high peak-to-average power ratio (PAPR), which may result in a low power amplifier efficiency [59]. Furthermore, the computational burden of performing the discrete Fourier transform (DFT) of the OFDM scheme increases with the number the TAs. Due to these reasons, the OFDM-based SM (OFDM-SM) schemes [60] and the related variants may not be suitable for the family LS-MIMO.

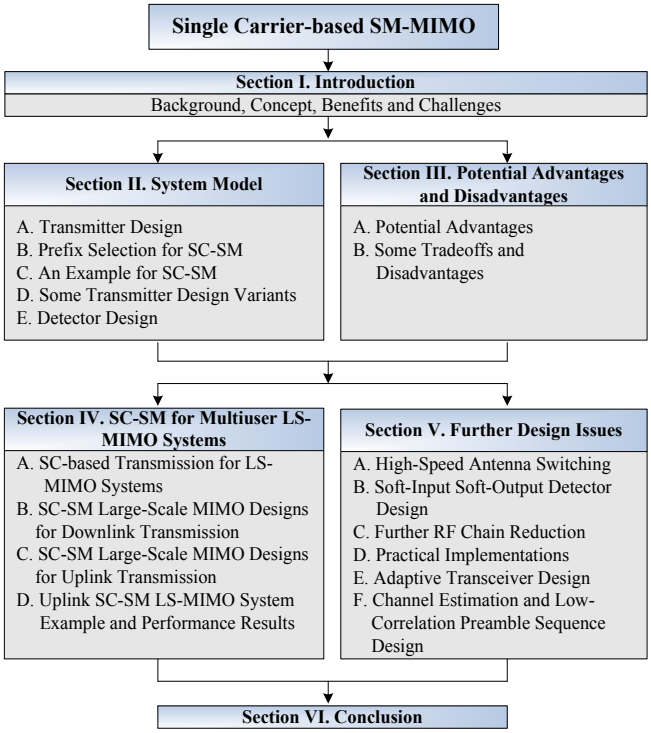

Fig. 1. Structure of this survey paper.

In recent years, the family of single-carrier (SC) or SC-like transmissions has become an interesting and promising alternative for LS-MIMO, which can reduce the complexity imposed by the DFT and has a lower PAPR than OFDM [61]–[64]. Moreover, as shown in [10], [65], the frequency-selective channel may be converted into a frequency-flat channel in LS-MIMO by carefully designed receive filters and therefore SC-based scheme can be directly used.

Motivated by the above-mentioned appealing characteristics of both SM and SC techniques shown in LS-MIMO transmissions, a flurry of research activities on SC-based SM (SC-SM) designs have been sparked off. In this paper we provide an overview of the broadband SC-SM architecture, which has the potential of exploiting the joint advantages of both SM and SC techniques. We summarize recent results concerning this novel transmission technique

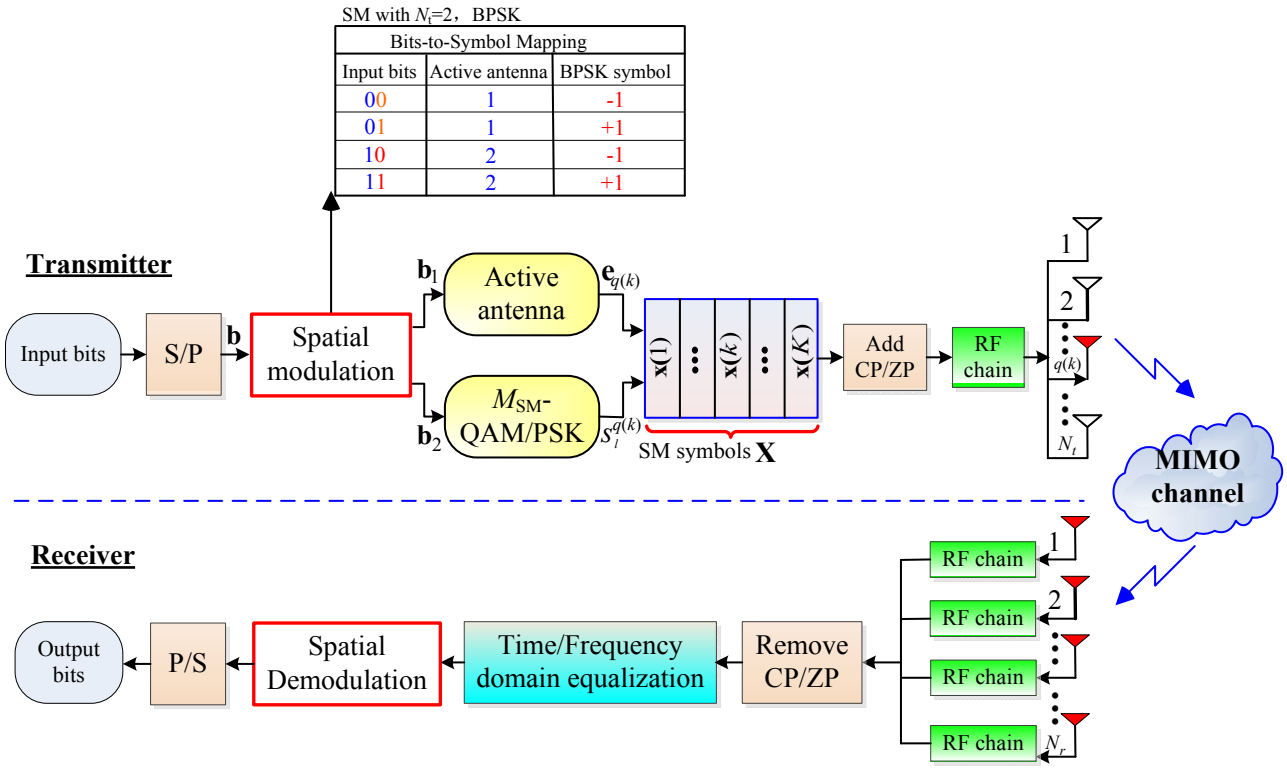

Fig. 2. General transceiver structure of SC-SM systems.

and outline the associated transceiver design, as well as a range of potential solutions in the scenario of LS-MIMO, highlighting its impediments as well as its future research directions to consider.

A. Outline

The remainder of this paper is organized as shown in Fig. 1. Section II introduces the system model of the SC-SM technique and its relevant variants, emphasizing the transmitter design, the prefix selection and various detector designs. In particular, both the time-domain and the frequency-domain as well as the associated turbo equalizers are investigated. The potential advantages and disadvantages of the SC-SM scheme are summarized in Section III. In Section IV the applications of the SC-SM transceiver to LS-MIMO systems are presented, where different SC-SM designs conceived for the multiuser LS-MIMO uplink and downlink are reviewed. Section V highlights a range of design issues that require more intensive study. Finally, Section VI concludes the paper.

B. Notations

The following notations are employed throughout this contribution. $(\cdot)^T$ and $(\cdot)^H$ denote the matrix transpose and Hermitian transpose, respectively. The probability of an event is represented by $p(\cdot)$. Furthermore, $\|\cdot\|$ and $|\cdot|$ denote the Euclidean norm and magnitude operators, while U is the number of users, N_{tot} is the number of antennas at the BS for its MU transmission and N_{u} is the number of antennas at each user for their multiuser transmission. Furthermore, N_t and N_r are the number of the antennas at transmitter and receiver for their point-to-point transmission, respectively, while M_{SM}, M_{VBLAST} and M_{STBC} are the sizes of the PSK/QAM constellation used in SM, space time block code (STBC) and vertical Bell labs layered space-time (VBLAST), respectively; K is the length of the transmission frame; $\mathbf{b}$ is the transmitted bit vector; $\mathbf{e}_i$ is the natural basis vector with only a single nonzero element at ith position; L is the maximum channel impulse response duration; ν is the length of the prefix of the transmit SC frame and $\mathbf{x}$ is the SM transmit symbol vector.

II. System Model of SC-SM

A. Transmitter Design

In this section, we consider a broadband SC-SM based MIMO system employing N_t TAs as well as N_r receive antennas (RAs) and communicating over a frequency-selective fading channel, as depicted in Fig. 2. In a conventional narrowband SM scheme, the information bits are conveyed by the indices of the TAs as well as the classic APM constellation (i.e. M_{SM}-PSK/QAM). Specifically, one of the N_t TA elements is activated at each time slot by $\log_2(N_t)$ information bits, while one of M_{SM}-APM symbols is selected by another $\log_2(M_{\text{SM}})$ information bits, which will be transmitted by the activated TA. In other words, the numbers of bits conveyed by the TA indices and APM symbols are $\log_2(N_t)$ and $\log_2(M_{\text{SM}})$, respectively.

In total, $m_{\rm SM} = \log_2(N_t M_{\rm SM})$ bits are sent over one SM symbol.

In broadband SC-SM, each SC transmit block is composed by the prefix part and the data part. The data part contains K SM symbols, each of which consisting of $m_{\rm SM}$ bits. Hence, a total of $m_r = Km_{\rm SM}$ bits are conveyed over an SC-SM symbol. We assume that there are L resolvable multipath links between each TA and RA pair, an $M_{\rm SM}$-PSK/QAM scheme is adopted, and N_t is a power of two[1]. Generally, in SC-SM based MIMO transmission [66], each transmit block can be generated by the following three steps:

Algorithm 1: Generation of a transmit frame according to SM mapping rule.

1) First, the information bit stream is divided into vectors containing $m_r = Km_{\rm SM}$ bits each, which will be transmitted over one SC-SM frame. Furthermore, each vector is split into K sub-vectors $\mathbf{b}(k), k = \{1, \cdots, K\}$ having length of $m_{\rm SM} = \log_2(N_t M_{\rm SM})$.
2) Next, each sub-vector $\mathbf{b}(k), k \in \{1, \cdots, K\}$ is mapped to an SM symbol. Specifically, based on the SM principle, each $\mathbf{b}(k)$ is divided into two sequences of $\log_2(N_t)$ and $\log_2(M_{\rm SM})$ bits, denoted by $\mathbf{b}_1(k)$ and $\mathbf{b}_2(k)$, respectively. The bits in $\mathbf{b}_1(k)$ are used for selecting a unique TA index $q(k)$ for activation, which is mapped to an N_t-dimensional natural basis vector $\mathbf{e}_{q(k)}$ (i.e., $\mathbf{e}_1 = [1, 0, \cdots, 0]^T$), while the bits in $\mathbf{b}_2(k)$ are mapped to an $M_{\rm SM}$-APM (i.e. PSK/QAM) constellation point $s_l^{q(k)}$. For simplicity, we refer to these two sets of bits as TA-bits and APM-bits. The resultant SM symbol based on the sub-vector $\mathbf{b}(k), k \in \{1, \cdots, K\}$ can be formulated by
$$\mathbf{x}(k) = [\underbrace{0, \cdots, 0}_{q(k)-1}, s_l^{q(k)}, \underbrace{0, \cdots, 0}_{N_t - q(k)}]^T \in \mathbb{C}^{N_t \times 1}, \quad (1)$$
where $q(k), k \in \{1, \cdots, K\}$ is the index of the activated TA during the kth interval. The corresponding transmit block of the K SM-mapped symbols is formulated as $\mathbf{X} = [\mathbf{x}(1), \cdots \mathbf{x}(k), \cdots, \mathbf{x}(K)]^T \in \mathbb{C}^{N_t \times K}$.
3) Finally, for each TA, a specific prefix vector $\mathbf{w} = [w(1), \cdots\cdots, w(\nu)]^T \in \mathbb{C}^{1\times\nu}$, i.e. the zero-padding (ZP) or cyclic prefix (CP) vector, is inserted for preventing the inter-block interference (IBI), which has to have a length larger than or equal to the maximum channel impulse response (CIR) duration L. Then, the SC-SM signal block and its prefix is transmitted over $(K + \nu)$ consecutive symbols durations.

The pseudo-code of Algorithm 1 is given in Table I. An example of conventional SM mapping rule for $N_t = 2$ employing BPSK modulation is portrayed in Fig. 2. In this system, the number of bits conveyed by each SM symbol is $m_{\rm SM} = \log_2(N_t M_{\rm SM}) = 2$. All possible two-bit combinations $\{00, 01, 10, 11\}$ are mapped to the TA indices $\{1, 2\}$ and to the BPSK constellation $\{-1, +1\}$, e.g. TA 1 is activated to transmit the BPSK constellation point -1 when the input bits are 00. According to **Algorithm 1**, at the receiver side, $\mathbf{y}(k) = [y_{k,1}, \cdots, y_{k,N_r}]^T$, where $y_{k,j}$ is the received signal on jth RA at time slot k, is given by
$$\mathbf{y}(k) = \sum_{l=0}^{L-1} \mathbf{H}_l \mathbf{x}(k-l) + \boldsymbol{\eta}(k), \quad (2)$$
where $\mathbf{H}_l$ is an N_r-by-N_t matrix with the entry h_{ij}^l being the lth CIR of the link spanning from the jth TA to the ith RA. Moreover, $\boldsymbol{\eta}(k) \in \mathbb{C}^{N_r \times 1}$ is the noise vector, whose elements are complex Gaussian random variables obeying $\mathcal{CN}(0, N_0)$. To elaborate a little further, we will provide an example of SC-SM in Section II-C.

[1]This restriction can be solved by the non-integer-based encoding method of [67] and the bit padding method of [68].

TABLE I
GENERATION OF AN SC-SM TRANSMIT FRAME ACCORDING TO SM MAPPING RULE.

Initialize:	SC-SM parameters N_t, N_r, $M_{\rm SM}$, L, $\mathbf{b}_I$, K, and $\mathbf{w}$
Step1:	Divide the input bit vector $\mathbf{b}$ into K sub-vectors $\mathbf{b}(k)$, having length of $m_{\rm SM} = \log_2(N_t M_{\rm SM})$ bits each.
Step2:	**For** $k = 1 : K$, **do**
	1) Split the sub-vector $\mathbf{b}(k)$ into $\mathbf{b}_1(k)$ and $\mathbf{b}_2(k)$
	2) Use $\mathbf{b}_1(k)$ to select a unique TA index $q(k)$
	3) Use $\mathbf{b}_2(k)$ to select an $M_{\rm SM}$-PSK/QAM constellation point $s_l^{q(k)}$
	4) Formulate the SM symbol for $\mathbf{b}(k)$ as $\mathbf{x}(k) = [\underbrace{0, \cdots, 0}_{q(k)-1}, s_l^{q(k)}, \underbrace{0, \cdots, 0}_{N_t - q(k)}]^T$
	end
	5) Form a transmit block $\mathbf{X}$ as $\mathbf{X} = [\mathbf{x}(1), \cdots \mathbf{x}(k), \cdots, \mathbf{x}(K)]^T$
Step3:	Insert the prefix $\mathbf{w} = [w(1), \cdots\cdots, w(\nu)]^T$ into $\mathbf{X}$.

B. Prefix Selection for SC-SM

As shown in Fig. 2, in order to suppress IBI, each SC block is extended by a guard interval, termed as the prefix vector. In conventional SC-based MIMO systems, the commonly adopted guard interval schemes may be roughly divided into four fundamental types [61], [62], as illustrated in Fig. 3, where both the attainable transmission rate and the power efficiency of an SC-based system are highly dependent on the specific type of the guard interval used.

- **CP scheme**: The last samples of each transmit block of K samples are copied to the beginning of this transmit block. Apart from the elimination of the IBI from the previous block, it also transforms the linear convolution of a frequency-selective multipath channel into a circular one and thus permits low-complexity channel diagonalization in the frequency domain at the receiver. However, the CP scheme suffers from a power efficiency reduction according to the factor of $K/(K + \nu)$.
- **ZP scheme**: A guard interval of samples is padded after each transmit block, during which no signal is

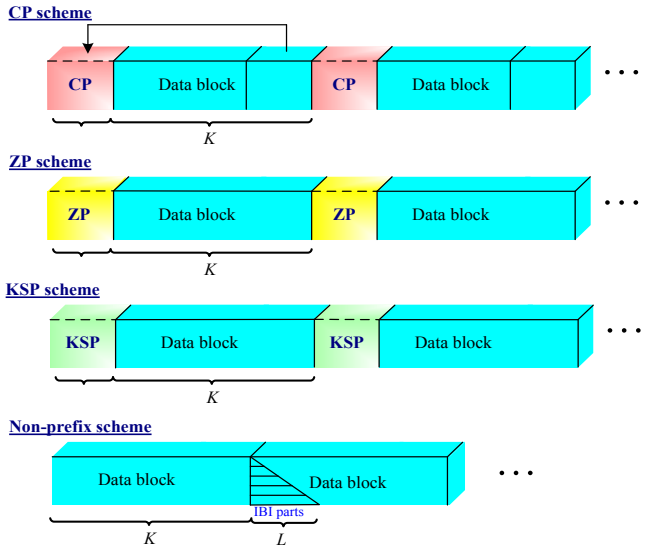

Fig. 3. Guard interval schemes for SC-based MIMO schemes in frequency-selective channels.

transmitted. It can avoid the power efficiency erosion of the CP scheme. Moreover, it supports a linear receiver in achieving full multipath diversity in some transmission scenarios [61]. The price paid is a somewhat increased receiver complexity.

- **Known symbol padding (KSP) scheme**: A guard interval consisting of a sequence of known samples is added after each transmit block. These known samples may represent a carefully designed sequence, such as a pseudo noise sequence [62]. In case of both CP and ZP schemes, data-aided channel estimation is performed by replacing some data symbols with pilot symbols, while the known symbols of KSP inserted into the guard interval can be directly used as pilot symbols. Note however that the KSP scheme also suffers from a power efficiency loss.
- **Non-prefix scheme**: The employment of the prefix vector imposes both a power and a spectral overheads, especially in case of a short channel coherence time and long CIR. To mitigate power and spectral overheads, the IBI can be reduced by using a powerful receiver even in the absence of a prefix vector, where iterative detection may be used. Moreover, to avoid the overhead imposed by the pilot signals, implicit training [69] can be adopted.

As a new SC-based MIMO technique, a suitable prefix vector should be carefully selected such that a specific SC-SM scheme can satisfy a diverse range of practical requirements. In [70], the authors exploited the classic CP scheme in the context of an SC-SM scheme and provided a diversity analysis framework. It was shown in [70] that the diversity order achieved by the CP-aided SC-SM under maximum-likelihood (ML) detection is only determined by the number of RAs N_r. Moreover, it was shown in [70] that their proposed SC-SM scheme is capable of outperforming its OFDM-based counterpart. However, the CP-aided SC-SM scheme suffers from a high detection complexity as well as a multipath diversity gain erosion. To be specific, in such a case, the ML complexity of this scheme is in the order of $O(N_t M_{\rm SM})^K$ and no multipath diversity gain can be achieved.

More recently, Rajashekar *et al.* [71] further generalized the solutions of [70], where a ZP-based SC-SM was proposed for reducing the order of ML detection complexity from $(N_t M_{\rm SM})^K$ to $(N_t M_{\rm SM})^L$, with L being the length of the CIR. Moreover, it was shown in [71] that the ZP-aided SC-SM scheme offers a full receive and multipath diversity order of LN_r and hence achieves significant performance improvement compared to both the CP-aided OFDM-SM and the CP-aided SC-SM schemes.

C. An Example for SC-SM

As an example, let us consider a (2×2)-element MIMO transmission ($N_t = N_r = 2$) associated with the throughput of $m_{\rm MIMO} = 4$ bits/channel-use (bpcu). We are interested in the comparison of SM with respect to other MIMO arrangements, such as the classic STBC and VBLAST schemes. In Fig. 4, five different MIMO schemes, namely SC-SM, OFDM-SM, SC-VBLAST, OFDM-VBLAST and OFDM-STBC, are considered. Note that in order to achieve the identical throughput, we consider 8-PSK, QPSK, and 16-QAM constellations for the SM-based, VBLAST, and the classic Alamouti STBC schemes [72], respectively. In all OFDM-based schemes, only the classic CP vector is inserted. For the sake of simplicity, we assume that the CIR length is $L = 3$ and the frame length is $K = 4$. Hence, the K MIMO symbols of a single frame convey a total of $(K \times m_{\rm MIMO}) = (4 \times 4) = 16$ bits. As shown in Fig. 4, the information bit stream is divided into sub-vectors containing 16 bits each. Assuming that the current transmit sub-vector is $\mathbf{b}$ =[1011001000101110], we present the details of the transmit vector generation of these five MIMO schemes as follows:

1) *SC-SM*: In SM, the throughput is $m_{\rm MIMO} = \log_2(N_t M_{\rm SM})$, which is achieved by using 8-PSK ($M_{\rm SM} = 8$) in our example in conjunction with $N_t = 2$. According to the SC-SM model detailed in Fig. 2, the sub-vector $\mathbf{b} = [1011001000101110]$ is further split into $K = 4$ sequences, i.e. $\mathbf{b}(1) = [1001]$, $\mathbf{b}(2) = [0000]$, $\mathbf{b}(3) = [1101]$, and $\mathbf{b}(4) = [1110]$. Then, each sequence $\mathbf{b}(k), k \in \{1, \cdots, 4\}$ is divided into $\log_2(N_t) = \log_2(2) = 1$ and $\log_2(M_{\rm SM}) = \log_2(8) = 3$ bits. Specifically, the sequence $\mathbf{b}(1) = [1001]$ is divided into $\mathbf{b}_1(1)$=[1] and $\mathbf{b}_2(1) = [001]$, $\mathbf{b}(2) = [0000]$ is divided into $\mathbf{b}_1(2)$=[0] and $\mathbf{b}_2(2) = [000]$, $\mathbf{b}(3) = [1101]$ is divided into $\mathbf{b}_1(3)$=[1] and $\mathbf{b}_2(3) = [101]$, and $\mathbf{b}(4) = [1110]$ is divided into $\mathbf{b}_1(4)$=[1] and $\mathbf{b}_2(4) = [110]$. Thus, the bits conveyed by the TA index are $\mathbf{b}_1 = [\mathbf{b}_1(1), \mathbf{b}_1(2), \mathbf{b}_1(3), \mathbf{b}_1(4)] = [1011]$ and the bits conveyed by 8-PSK signals are $\mathbf{b}_2 = [\mathbf{b}_2(1), \mathbf{b}_2(2), \mathbf{b}_2(3), \mathbf{b}_2(4)] = [001000101110]$. After this split, $\mathbf{b}(k), k \in \{1, \cdots, 4\}$ are mapped to the conventional SM symbols. For example, for the

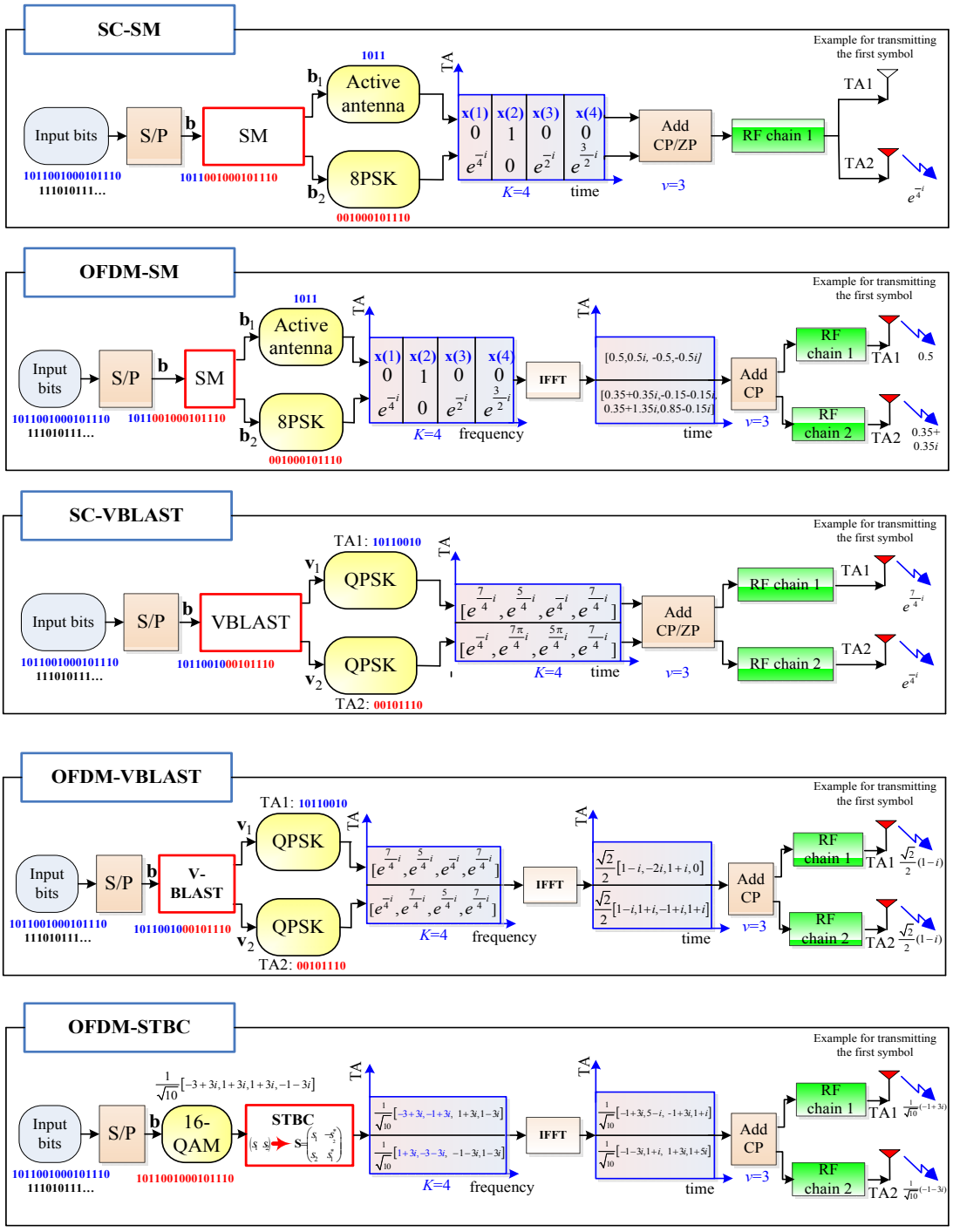

Fig. 4. Examples of different MIMO transmitters for multipath channels at a throughput of 4 bits/channel-use, where the SC-SM, the OFDM-SM, the SC-VBLAST, the OFDM-VBLAST and the OFDM-STBC schemes are considered.

sequence $\mathbf{b}(1) = [\mathbf{b}_1(1), \mathbf{b}_1(2)]$, $\mathbf{b}_1(1)$=[1] is used to activate TA 2 and $\mathbf{b}_2(1) = [001]$ is mapped to the 8-PSK constellation point $e^{\frac{\pi}{4}i}$, which is transmitted over TA 2. Hence, the corresponding SM symbol for transmission is $\mathbf{x}(1) = [0, e^{\frac{\pi}{4}i}]^T$. Similarly, we can also generate the transmit SM symbols $\mathbf{x}(2)$, $\mathbf{x}(3)$ and $\mathbf{x}(4)$ corresponding to $\mathbf{b}(2)$, $\mathbf{b}(3)$ and $\mathbf{b}(4)$, respectively. The resultant SC-SM transmit frame is formulated by $\mathbf{X} = [\mathbf{x}(1), \mathbf{x}(2), \mathbf{x}(3), \mathbf{x}(4)]^T$. Finally, the ZP or CP vector is inserted by using the method shown in Fig. 3.

2) *OFDM-SM*: The initial bit-to-symbol mapping process of OFDM-SM is the same as that of the SC-SM scheme, except that the transmit signal $\mathbf{X}$ is considered to be a frequency-domain signal and an inverse fast Fourier transform (IFFT) unit is used to produce the corresponding complex-valued time-domain signal, e.g., the frequency-domain vector

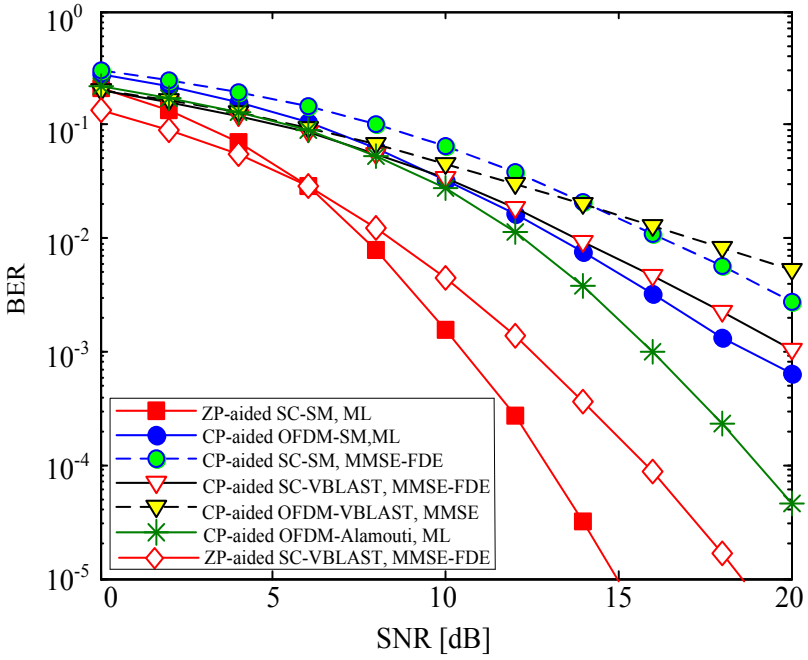

Fig. 5. BER comparison of the ZP-aided SC-SM scheme over its CP-aided counterpart and various CP-aided classic MIMO transmission schemes. All the schemes are assumed to have $N_t = 2$, $N_r = 2$ and the identical throughput $m_{\text{SM}} = 4$ bits/channel-use. Both SC and OFDM techniques are considered. ML as well as the MMSE-type detectors are employed.

[0 1 0 0] transmitted over TA 1 is converted to its time-domain signal as $[0.5, 0.5i, -0.5, 0.5i]$. As shown in Fig. 4, the OFDM-SM signal generated is no longer sparsely distributed in the spatial domain and two TAs (two RF chains) have to be simultaneously activated over the OFDM frame. Fig. 4 shows an example of the OFDM-SM signal transmission for the first symbol of $[0.5, 0.35 + 0.35i]$.

3) *SC-VBLAST*: In VBLAST, each TA simply transmits an independent symbol stream and the throughput is $m_{\text{MIMO}} = N_t \log_2(M_{\text{VBLAST}})$, where M_{VBLAST} represents the order of APM constellation by the VBLAST scheme. In our example associated with $m_{\text{MIMO}} = 4$ bpcu and $N_t = 2$, we have $M_{\text{VBLAST}} = 4$ and hence a QPSK modulation is used. As shown in Fig. 4, the bit partitioning of the input bit stream $\mathbf{b} = [1011001000101110]$ is different from that in SM. Specifically, $\mathbf{b}$ is first equally partitioned into two sub-vectors $\mathbf{v}_1 = [10110010]$ and $\mathbf{v}_2 = [00101110]$ and then further divided into $K = 4$ sequences. For example, $\mathbf{v}_1 = [10110010]$ is split into $[10], [11], [00]$ and $[10]$, which will be mapped to the QPSK symbols of $e^{\frac{7\pi}{4}i}$, $e^{\frac{5\pi}{4}i}$, $e^{\frac{\pi}{4}i}$, $e^{\frac{7\pi}{4}i}$, respectively. The transmited SC-VBLAST vector of TA 1 is given by $[e^{\frac{7\pi}{4}i}, e^{\frac{5\pi}{4}i}, e^{\frac{\pi}{4}i}, e^{\frac{7\pi}{4}i}]$. The same process can be carried out for TA 2. Finally, the ZP or CP vectors for the generated transmit vector of each TA are inserted.

4) *OFDM-VBLAST*: Based on the signal generation steps of SC-VBLAST, we need to add an IFFT unit to produce the OFDM-VBLAST transmit signal, as shown in Fig. 4. After this, such a signal will be sent out over multiple sub-carriers, which are orthogonal to each other.

5) *OFDM-STBC*: The throughput of STBC depends on its code rate (or the multiplexing gain) c_{STBC} and is given as $m_{\text{MIMO}} = c_{\text{STBC}} \log_2(M_{\text{STBC}})$, where M_{STBC} is the order of the APM used by the STBC scheme. In our example associated with $N_t = 2$, the classic Alamouti STBC with $c_{\text{STBC}} = 1$ is used and 16-QAM ($M_{\text{STBC}} = 16$) is employed to achieve the target throughput of $m_{\text{MIMO}} = 4$ bpcu. In contrast to the VBLAST and SM schemes, the input bit stream $\mathbf{b} = [1011001000101110]$ is directly mapped to four 16-QAM symbols as in $\frac{1}{\sqrt{10}}[-3 + 3i, 1 + 3i, 1 + 3i, -1 - 3i]$. Then, the Alamouti encoding matrix is applied to every pair of symbols and an IFFT unit converts the frequency-domain signal into its time-domain counterpart.

Based on the transmit models of Fig. 4, we compared the BER performance of SC-SM schemes against that of the conventional MIMO schemes in Fig. 5 over Rayleigh fading channels having a uniform power delay profile [71]. In this context, several commonly used detectors are considered, i.e. ML detector, single-tap based minimum mean-squared error (MMSE) detector or MMSE based frequency-domain equalization (FDE) [66], [70], [71].

As shown in Fig. 5, the ZP-aided SC-SM scheme using the ML detector is capable of achieving a considerable diversity gain and hence it attains the best BER performance amongst all benchmark schemes. As pointed out in in [62], the ZP-type prefix vector results in a better BER compared to its CP counterpart, since in the latter case any data detection errors may affect both the information

TABLE II

COMPLEXITY ORDERS AND THE NUMBER OF RF CHAINS REQUIRED FOR DIFFERENT ZP-AIDED AND CP-AIDED MIMO SCHEMES.

Scheme	Detector	Complexity Order (Flops)	RF Chains
ZP-aided SC-VBLAST	ML	$\mathcal{O}((M_{\text{VBLAST}})^{N_t L})$	N_t
	MMSE	$\mathcal{O}(L^3 N_r^3 N_t K) + \mathcal{O}(L^3 N_r N_t^3 K) + \mathcal{O}(L^3 N_r^2 N_t^2 K)$	N_t
CP-aided SC-VBLAST	MMSE-FDE	$\mathcal{O}(N_r N_t^2 K) + \mathcal{O}(N_t^3 K) + \mathcal{O}(N_t K^2) + \mathcal{O}(N_t^2 K M_{\text{VBLAST}})$	N_t
CP-aided OFDM-VBLAST	ML	$\mathcal{O}(N_r (M_{\text{VBLAST}})^{N_t} K)$	N_t
	MMSE	$\mathcal{O}(N_t^2 N_r K) + \mathcal{O}(N_t^3 K)$	N_t
CP-aided OFDM-STBC	ML	$\mathcal{O}(N_t N_r^2 K)$	N_t
CP-aided SC-SM	ML	$\mathcal{O}((N_t M_{\text{SM}})^K)$	1
	MMSE-FDE	$\mathcal{O}(N_r N_t^2 K) + \mathcal{O}(N_t^3 K) + \mathcal{O}(N_t K^2) + \mathcal{O}(N_t^2 K M_{\text{SM}})$	1
CP-aided OFDM-SM	MMSE	$\mathcal{O}(N_r N_t^2 K) + O(N_t^3 K)$	N_t
ZP-aided SC-SM	ML	$\mathcal{O}((N_t M_{\text{SM}})^L)$	1
	LSS	$\mathcal{O}(N_t^2 M_{\text{SM}} M K) + \mathcal{O}(L K N_t N_r M)$	1

M_{VBLAST}: the APM order used in VBLAST scheme.
M_{SM}: the APM order used in SM scheme.
L: the length of the CIR.
M: the selected M value in the near-ML LSS detector.
K: the length of the frame.
N_t: the number of transmit antennas.
N_r: the number of receive antennas.

symbols and the CP symbols. In this comparison, we only consider a small frame length K for illustration purpose. In [71] and [88], more comparisons of the SC-SM schemes over other MIMO schemes are provided for larger K, in which the afore-mentioned BER benefits were also observed.

Moreover, in Table II, the complexity orders of different ZP-aided and CP-aided MIMO schemes are compared, where only the multiplications of complex numbers are counted. The complexity orders of different detectors for OFDM-SM, OFDM-STBC and OFDM-VBLAST schemes can be found in [16], while that of the other MIMO schemes can be found in [71] and [88]. In Table II, we also provide the complexity order of the near ML detector, namely low-complexity single-stream (LSS) detector [88], for the promising ZP-aided SC-SM. The details about the near-ML LSS detector will be further discussed in Section II-D. As shown in Table II, the CP-aided MIMO systems with the MMSE and the MMSE-FDE based detectors exhibit lower complexity orders compared to those of ZP-aided MIMO systems with time-domain detectors (ZP-aided SC-VBLAST with MMSE detector and ZP-aided SC-SM with LSS detector), since these CP-aided systems can use low-complexity one-tap equalizations. However, as shown in our simulation results, CP-aided MIMO systems suffer from a multipath diversity gain loss. As proved in [71], the ZP-aided SC-SM scheme with ML detector is capable of offering full multipath diversity and hence exhibits better BERs shown in Fig. 5. This benefit can also be achieved by using the LSS algorithm proposed in [88], as will be shown in Figs. 7 and 8 in Section II-D.

By taking into account both the BER and the complexity, we conclude that ZP-aided SC-SM is a promising candidate for dispersive MIMO channels. Note that the detection complexity of ZP-aided SC-SM may be further reduced by exploiting the spatial-domain sparsity of SM symbols, as discussed in [88] and Section III. Moreover in Table II, we also provide the number of RF chains required for different MIMO schemes in dispersive channels. It is shown in Table II that the SC-SM schemes require only a single RF chain at the transmitter.

Note that although the above-mentioned research demonstrated that the ZP based scheme constitutes a promising prefix option, further investigations are required to strike an attractive tradeoff amongst the detection complexity imposed, the attainable BER, as well as the achievable transmission rate and power efficiency.

D. Some Transmitter Design Variants

In recent years, diverse generalized SM schemes have been proposed, such as the GSM of [73]–[75], the SSK scheme of [37], and the GSSK arrangements of [76], [77]. However, these schemes have been predominantly investigated in the context of narrow-band scenarios, assuming that SM symbols are transmitted over flat-fading channels. However, in practice, most of the wireless channels exhibit frequency selective properties. This leads to several further generalized SM versions, which aim to provide increased transmission rate, improved the energy efficiency or higher multipath diversity gain [78]–[80]. Explicitly, there are three types of SC-SM variants: the SC-GSM scheme [78], the space and time-dispersion modulation (STdM) scheme [79] and the family of SFSK arrangements [80], which are detailed as follows:

- **SC-GSM**: As a natural extension of SM, the GSM scheme was proposed in [81] for the sake of achieving increased-rate data transmission, which activates several TAs— rather than a single TA or all TAs — to carry the information symbols during each time slot. Specifically, in GSM, N_g out of N_t ($N_g < N_t$)

TAs are activated during each time slot, where the information bits are conveyed both by the active TA-index combinations as well by the N_g conventional APM symbols [82]. This extension has also been incorporated into SC-based transmission over dispersive channels, where the single-RF restriction is relaxed by using N_g RF chains [78]. In general, SC-GSM includes SC-SM as a special case associated with $N_g = 1$, which strikes a trade-off among the transmit rate, the RF cost as well as the detection complexity.

- **STdM**: By exploiting the principle of SM in both time-dispersion and space dimensions, an STdM scheme was proposed for frequency selective fading channels in [79], where the channel's time-slot indices are exploited for conveying additional information, apart from the active TA index and the conventional APM symbols of SM. In contrast to conventional SC-SM scheme, STdM exploits the resolvable multipath components of the frequency-selective channel as a novel means of conveying additional source information. Specifically, in the STdM scheme, only one out of N_t TAs was activated in one out of $L-1$ resolvable multipath components, where L is the CIR length. In [79], the energy efficiency of STdM was evaluated based on a realistic power consumption model and it was found to be more energy-efficient than SC-SM. Note that the design of STdM critically hinges on the idealized assumption that independent symbol-spaced taps are available for MIMO channels.
- **SFSK**: In [80], by intrinsically amalgamating the concept of SM and linear dispersion codes (LDCs) [83], Ngo *et al.* proposed the design philosophy of SFSK, which selects one out of φ orthogonal frequencies by a frequency shift keying (FSK) modulator. In contrast to the TA-index in conventional SM, in SFSK, the specific indices of the pre-designed space-time dispersion matrices are exploited for conveying extra implicit information. Moreover, this concept was further extended in [80] to enjoy benefits offered by the time, space and frequency domains. SFSK may be viewed as an SC-based transmission scheme, because only a single frequency tone (out of multiple carriers) is utilized in each transmission. Note that the transmission of space-time dispersion matrix requires multiple RF chains and the advantages of single-RF are eroded, except for the low-rate designs of [2].

E. Detector Design

Traditional receiver architectures designed for conventional SM and classic MIMO schemes may not be directly suitable for the family of SC-SM, due to the following reasons:

(1) Conventional SM detectors of [19], [84], [85] are focused on the detection of the TA index and APM symbol in flat-fading scenarios, which usually ignore the inter-symbol interference (ISI) caused by the channel's frequency selectivity.

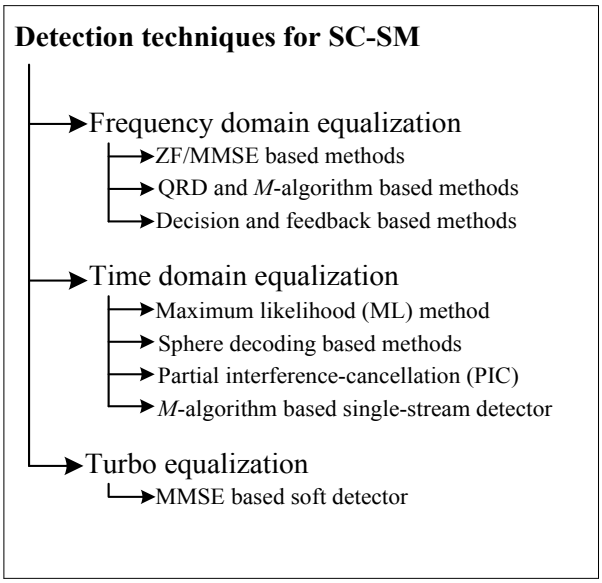

Fig. 6. Overview of SC-SM detectors.

(2) Most of the existing MIMO detectors conceived for multipath fading channels are proposed under the assumption that the MIMO channel matrix has column full-rank ($N_r \geq N_t$) [58], [86]. However, an attractive advantage of SM is that it can efficiently operate also in the challenging scenario of asymmetric/unbalanced MIMO systems, whose channel matrices may be rank-deficient due to having more TAs than RAs.

This inspired recent research efforts in devising sophisticated receivers for SC-SM systems. At the time of writing, there are three typical receiver architectures: frequency-domain equalizer (FDE) [66], [87], time-domain equalizer (TDE) [70], [71], [88] and the powerful turbo equalizer (TEQ) [87]. A sketch of these detection techniques conceived for SC-SM systems is provided in Fig. 6. Next, they will be characterized in a little more detail.

1) Frequency-Domain Equalizer: An attractive low-complexity approach to ISI mitigation, in scenarios exhibiting a long CIR, affecting thousands of bits is constituted by FDEs, because we can rely on single-tap frequency-domain channel transfer factor (FDCHTF) instead of a time-domain equalizer having thousands of taps. Hence, SC systems using FDEs (SC-FDE) have been adopted in some recent communication standards, such as the third generation partnership project (3GPP) long-term evolution (LTE) standard. The benefits of SC-FDE also have been explored in the context of various MIMO techniques. A detailed overview of SC-FDE techniques was presented in [62], [89] and both the MMSE-based FDEs and the decision-feedback equalizer (DFE) based FDEs were introduced. As a novel MIMO technique, SM may also be beneficially combined with SC-FDE methods for combating the effects of ISI.

To this end, in [66] various state-of-the-art FDE algorithms conceived for VBLAST were investigated in the context of CP-aided SC-SM systems. Specifically, the zero

forcing (ZF)-based FDE of [90], the MMSE-based FDE (MMSE-FDE) of [91], and the decision feedback based approaches [62] as well as the QR decomposition combined with the M-algorithm (QRD-M) [62] were utilized to recover the transmit vector, in which an SM signal vector was viewed as a special type of the VBLAST signal. Then, the low-complexity matched filter (MF) based detection method of [16] was utilized, where the activated TA index and the modulated APM constellation point are separately estimated. That detector directly combines the classic VBLAST detector conceived for ISI channels and the MF-based detector of conventional SM schemes for demodulation. It was shown in [66] that the QRD-M detector outperforms other detectors in the context of SC-SM systems, since it was designed based on the near-optimal tree search principle by selecting only M most possible survived branches [92]. Moreover, in [87] the authors exploited the MMSE criterion to derive the weights of the FDE for the CP-aided SC-SM. Similar to the classic MMSE-FDE, the received signals were first converted to their frequency-domain versions and then MMSE-based linear filtering was invoked for estimating the frequency-domain SC-SM signals by minimizing the average minimum square error between the frequency-domain signals and the estimates. Then, these estimates were converted to their time-domain counterparts, which were further divided into several independent SM symbols. Finally, the single-stream symbol-based ML detector of [84] was employed to each SM symbol for jointly detecting both the active TA index as well as the transmitted APM symbol. In contrast to the classic equalizers designed for traditional MIMO systems, it was found in [87] that their MMSE-based FDE taps depend on the sparsity of the SM symbols. In short, this detector first employs a carefully designed MMSE-FDE for generating an initial estimate and then invokes the conventional single-stream ML detector of SM for symbol-by-symbol detection. As shown in [87], the complexity of this detector is independent of the CIR length. However, most of the above-mentioned FDE algorithms are only suitable for scenarios, where the channel matrix is of full-rank, i.e. $N_r \geq N_t$.

2) Time-Domain Equalizer: A well-known classic approach to ISI-mitigation in the SC-based systems is based on the employment of a TDE. Various TDE methods [62], such as the ML-based TDE, the low-complexity linear TDE, the parallel interference cancellation (PIC), as well as the successive interference cancellation (SIC) have been extensively studied in the context of MIMO systems. In contrast to the transmitted signals generated by conventional MIMO schemes, the transmit vectors of SM schemes are sparsely populated, since typically only a single TA is activated [18], [19]. This constraint makes SM rather different from the classic STBC or the VBLAST schemes [1] and the TDE of SC-SM has to be carefully designed for exploiting the benefits of both SC and SM techniques.

In [70], an optimal ML detector was proposed for SC-SM schemes, which carries out an exhaustive search for finding the global optimum in the entire transmit signal space. This detector jointly detects the entire transmission frame to retrieve the original m_r bits. The advantages of the ML detector over the ZF and the MMSE detectors were evaluated for the CP-aided SC-SM schemes. However, as both the transmission rate and K increase, the complexity of the ML detector becomes excessive.

To attain a high diversity gain, in [71] a ZP-aided SC-SM scheme was investigated. To reduce its detection complexity, the authors viewed this system as a new kind of STBC scheme, which allows the use of STBC's generalized distribution law (GDL) to simplify the corresponding ML detector. It was found that the order of the ML detection complexity in the ZP-aided SC-SM scheme only depends on the CIR length rather than on the frame length K, as mentioned in Section II-B. To further reduce the complexity imposed by a large value of L, a low-complexity PIC-based receiver with SIC (PIC-R-SIC) was proposed in [71], which is capable of achieving both multipath- and receiver- diversity gains (compared to ML detector) for some specific channel conditions. Compared to the conventional PIC-R-SIC designed for STBC schemes operating in a flat-fading scenario, the extended PIC-R-SIC detector is suitable for a dispersive channel, which operates by converting the dispersive multipath channel into a set of frequency-flat block fading subchannels.

Another promising method of reducing the complexity of the ML detector is constituted by the sphere decoding (SD) algorithms of [93], the concept of which is to search for the closest lattice points within a certain SNR-dependent search radius. However, the number of surviving search paths is still relatively high for a large tree and it may only be suitable for SC-SM schemes having a small frame length K.

Relying on the concept of the classic M-algorithm, in [88] the authors proposed a low-complexity single-stream (LSS) detector for avoiding the channel inversion operation of the PIC-R-SIC scheme, while striking a flexible trade-off between the computational complexity imposed and the attainable BER. Note that in the traditional M-algorithm, the QR-decomposition requires the channel matrix to be a full-rank (column-wise) matrix. Hence, it can not be directly applied by the ZP-aided SC-SM, where the channel matrix may be rank deficient. In the proposed LSS, the QR-decomposition is avoided by properly exploiting the single-stream ML detection of [84]. It was found that their proposed LSS detector is also capable of efficient operation in the challenging rank-deficient channel scenarios.

3) Turbo Equalizer: It is worth noting that nearly all wireless communication systems employ some forms of forward error correction (FEC) to counteract unpredictable transmission errors, which require soft-decision based detectors rather than the hard-decision based TDE and FDE. The classic TEQ [94] has also been demonstrated to be an effective soft-decision receiver in frequency selective fading channels, incorporating both equalization and channel decoding. The basic concept of TEQ relies

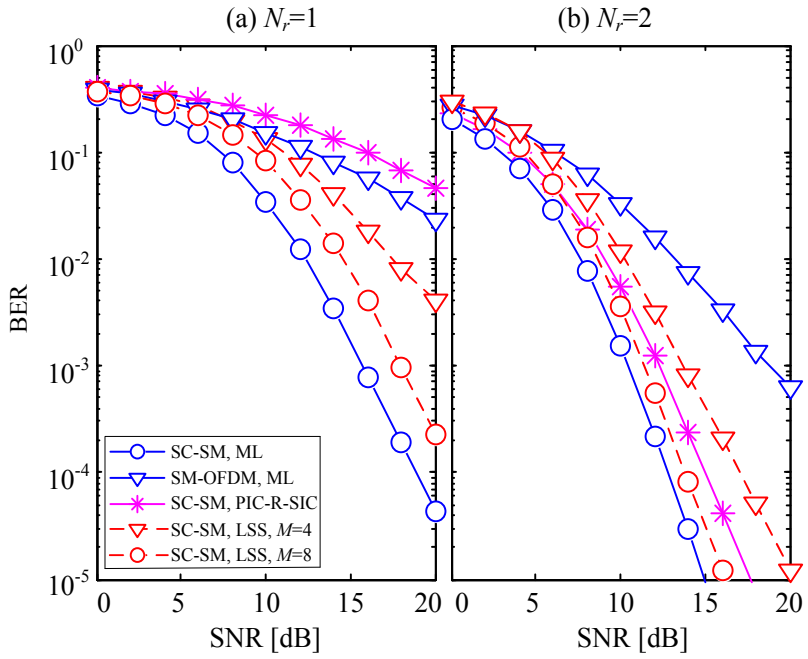

Fig. 7. BER performance of the ZP-aided SC-SM schemes employing the ML, the parallel interference cancellation (PIC)-based receiver with successive interference cancellation (SIC) (PIC-R-SIC) and the LSS based receivers for transmission over dispersive multipath channels. The identical-throughput CP-aided OFDM-SM schemes of [16] employing an ML-based receiver are considered as benchmarkers. All the systems are assumed to have $N_t = 2$, $K = 4$, $L = 3$, $m_{\mathrm{SM}} = 4$ bpcu and using an 8-PSK constellation.

on the iterative exchange of soft information in the form of log-likelihood ratios (LLRs), between the equalizer and the decoder. The trellis-based TEQ relying on the Viterbi algorithm and the Bahl-Cocke-Jelinek-Raviv (BCJR) algorithm [94] imposes high complexity in the context of SC-MIMO systems, especially for high CIR lengths L and for a large APM size M_{SM}. Hence, the low-complexity yet efficient MMSE-based TEQ is the one that is commonly used.

Recently, in [87] an MMSE based low-complexity soft-decision FDE algorithm was developed for broadband high-rate SC-SM systems, which is capable of operating in dispersive channel having a long CIR. Specifically, they first proposed a hard-decision aided SC-SM detector based on the MMSE criterion and then developed its soft-decision version by employing maximum *a posteriori* (MAP) demodulation. The MMSE-FDE coefficients obtained are different from those derived for traditional MIMO schemes, because every SM symbol exhibits sparsity. Moreover, in [87] a three-stage concatenated SC-SM architecture was proposed for attaining a near-capacity performance by amalgamating a recursive systematic convolutional code and a unity-rate convolutional code, which was achieved by exchanging the extrinsic information of these decoders a sufficiently high number of times, until no more iteration gains were achieved. Effectively, this resulted in a two-stage system. Similar to the above-mentioned FDE detectors, this detector was also designed under the constraint of $N_r \geq N_t$.

Note that most of the above-mentioned detectors assume that perfect channel state information (CSI) is available at the receiver. However, it is challenging to acquire accurate CSI, which results in a severe degradation of the achievable performance. This effect has been theoretically analyzed in narrowband SM systems. In order to dispense with CSI-estimation, some differential SM schemes have been proposed in flat-fading scenarios [18]. However, these investigations have not been extended to SC-SM. This issue will be further discussed in Section V-F.

4) Performance: The observations above have shown that the TDE-type detectors may be more attractive in the context of SC-SM, since they are capable of retaining all the benefits of SC and SM techniques. They are also suitable for arbitrary antenna configurations, including the scenarios of $N_r \leq N_t$. Fig. 7 characterizes the BER performance of the ZP-aided SC-SM schemes in the context of (2×1) and (2×2) MIMO channels at a throughput of $m_{\mathrm{SM}} = 4$ bpcu for transmission over Rayleigh multipath channels having a uniform power delay profile [71]. To evaluate the performance gaps between the low-complexity sub-optimal detectors and ML detector, we first consider a small frame length K in our simulations and then adopt a higher value of K. To be specific, in Fig. 7, similar to the setup of [71], the frame length is set to $K = 4$ and the 8-PSK constellation is adopted, the CIR length is $L = 3$ and different TDE algorithms are considered. We also consider the identical-throughput CP-aided OFDM-SM schemes of [16] as benchmarkers.

Observe in Fig. 7 (a) that the LSS detector performs well in rank-deficient (2×1)-element MIMO channels, while the PIC-R-SIC method suffers from a multipath diversity reduction. For (2×2) MIMO channels, the LSS detector

TABLE III
COMPLEXITY ORDERS OF DIFFERENT TIME-DOMAIN DETECTORS FOR ZP-AIDED SC-SM SCHEME.

Detector	Complexity Order (Flops)
ML	$\mathcal{O}((N_t M_{\mathrm{SM}})^L)$
PIC-R-SIC	$O(N_t^2 K^2 N_r) + O(K^3 N_t) + O((K+L)N_t^2 M_{\mathrm{SM}} K)$
LSS	$\mathcal{O}(N_t^2 M_{\mathrm{SM}} M K) + \mathcal{O}(LKN_t N_r M)$

TABLE IV
COMPLEXITY OF DIFFERENT DETECTORS FOR ZP-AIDED SC-SM SCHEME IN TERMS OF THE NUMBER OF REAL-VALUED MULTIPLICATIONS, WHERE THE SETUP IS THE SAME AS THAT IN FIG. 7.

$N_t=2$, $K=4$, $L=3$, 8-PSK				
Detector	ML	PIC-R-SIC	LSS	
			$M=4$	$M=8$
N_r=1	1.3×10^7	1.0×10^4	5.4×10^3	1.1×10^4
N_r=2	2.7×10^7	2.5×10^4	1.1×10^4	2.1×10^4

TABLE V
COMPLEXITY OF THE PIC-R-SIC AND LSS DETECTORS FOR ZP-AIDED SC-SM SCHEME, WHERE THE SETUP IS THE SAME AS THAT IN FIG. 8.

$N_t=32$, $K=128$, $L=6$, QPSK			
Detector	PIC-R-SIC	LSS	
		$M=4$	$M=8$
N_r=2	5.9×10^{12}	1.4×10^9	2.2×10^9
N_r=4	7.6×10^{12}	2.2×10^9	4.3×10^9

having $M = 8$ outperforms the PIC-R-SIC method and provides a signal-to-noise ratio (SNR) gain of about 1.6 dB at the BER of 10^{-5}. Moreover, in Fig. 7(b) the performance gap between the LSS detector and the exhaustive-search-based ML detector is only about 5 dB and 1 dB for $M = 4$ and $M = 8$, respectively. This gap can be further reduced by setting a larger value of M at the cost of a higher complexity. In general, the LSS detector is capable of adjusting the parameter M for striking a flexible tradeoff between the attainable BER and the detection complexity imposed.

The above-mentioned benefits of the LSS detector recorded for the ZP-aided SC-SM are also visible in Fig. 8, where a long frame length of $K = 128$ and a large number of TAs, namely $N_t = 32$ are considered in the extended vehicular *a* channel (EVA) model [90]. In Fig. 8, the BER performance of the optimal ML detector is not provided due to its excessive complexity. It is shown in Fig. 8 that the BER of the PIC-R-SIC scheme may have an error floor effect under rank-deficient channel conditions, which was also observed in [88].

5) Complexity: In Table III, the complexity orders of the PIC-R-SIC, the ML and the LSS detectors employed in Figs. 7 and 8 are compared. It is shown that the complexity of the ML detector is unaffordable as it grows exponentially with the CIR length L. Based on the results of Tables II and III, it is noted that the time-domain based LSS detector has a similar complexity order to that of the classic linear MMSE based detector. In Tables IV and V, we also provide the approximate complexity of the configurations adopted in Figs. 7 and 8. It is shown that the LSS detector is capable of striking a flexible tradeoff in terms of the BER attained and the complexity imposed by adjusting the parameter M.

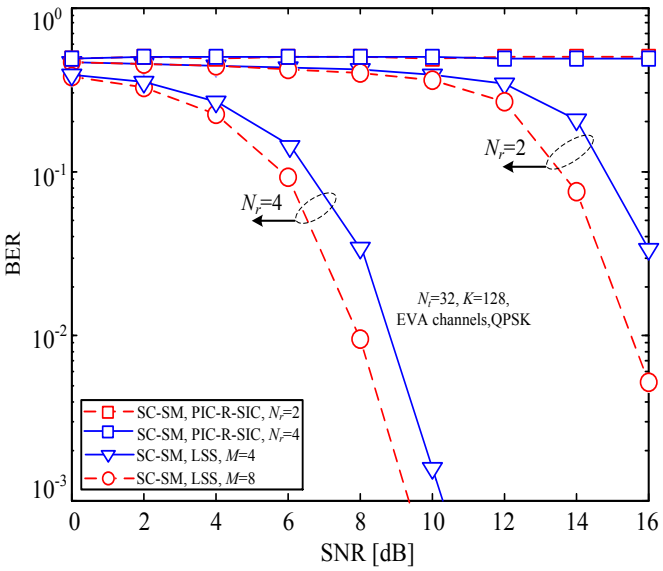

Fig. 8. BER performance of the ZP-aided SC-SM schemes employing the PIC-R-SIC and the LSS based methods for transmission over the EVA channels, having $L = 6$, QPSK modulation and $N_r = 2, 4$. Here, the performance of these detectors with a higher number of TAs $N_t = 32$ and a longer frame length $K = 128$ are investigated, compared to Fig. 7.

III. POTENTIAL ADVANTAGES AND DISADVANTAGES

In light of the transceiver design described in Section II, we summarize some potential advantages, tradeoffs and disadvantages of SC-SM in Fig. 9.

A. Potential Advantages

1) ***Simple Transmitter Design****:* In conventional MIMO systems, such as the VBLAST and the STBC schemes, the hardware complexity and cost rise with the number of TAs N_t. Moreover, the deleterious effects of RF circuit mismatches and coupling impairments also grow with the value of N_t. These factors limit the number of antennas. As shown in Fig. 2, SC-SM relies on the unique encoding philosophy of activating one out of numerous TAs at each time slot, hence only a single RF chain (N_g RF chains for the SC-GSM scheme, $N_g < N_t$) is required instead of N_t parallel RF chains. Hence its RF section has a reduced complexity and cost. On the other hand, in conventional OFDM-based MIMO transmissions, the complexity imposed by performing the DFT operations for its signal modulation and demodulation also increases

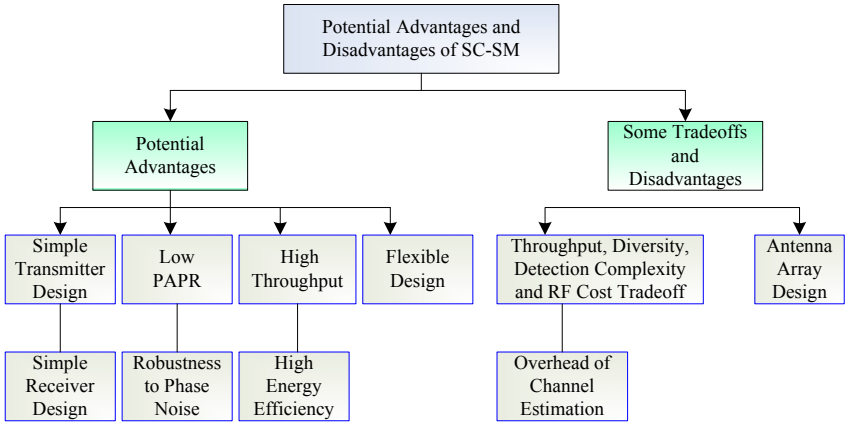

Fig. 9. A summary of main advantages and disadvantages of the SC-SM scheme.

with N_t. As shown in Section II and Fig. 2, this computational complexity and the RF hardware complexity can be reduced by employing the SC-SM based transmitter advocated.

*2) **Simple Receiver Design**:* Data detection in the conventional MIMO systems is one of the most challenging tasks in terms of both its computational complexity and its power consumption, especially in the LS-MIMO scenarios. In dispersive channels, the employment of SC or OFDM techniques further increases the dimensionality of the underlying detection problem. In SM, since only a single TA is activated for transmission, this allows us to design a low-complexity single-stream receiver, such as the LSS detector. Moreover, based on the unique bit-to-vector mapping rule of SC-SM detailed in **Algorithm 1**, the transmit vector of SC-SM associated with each TA has as low a fraction of nonzero elements as K/N_t for each row of $\mathbf{X}$. Usually, a matrix or vector is referred to as sparse, if the number of nonzero elements in it is less than 20% of the total number of elements. Since the sparsity ratio of SC-SM is $1/N_t$, for $N_t > 4$ the transmit matrix $\mathbf{X}$ is deemed sparse and hence the detection can be regarded as a sparse reconstruction problem. Therefore, the classic sparse reconstruction theory [95], [96] may be invoked for recovering the transmitted signals.

Accordingly, a number of related contributions have concentrated on the design of SM detection schemes based on compressive sensing (CS). A message passing detection algorithm was proposed in [105] for the multiple access channel (MAC) in conjunction with a high number of antennas at the BS. An iterative detector was developed for large-scale MACs in [106], where the authors decoupled the antenna and symbol estimation processes for reducing the total detection complexity. The algorithm introduced in [112] beneficially exploits the sparsity of SM transmission in the MAC. In [107], a generalized approximate message passing detector was preferred to the high-complexity stage-wise linear detector. A closely related approach has also been developed in [113] in order to mitigate the effects of spatial correlation imposed on tightly-packed antennas.

*3) **Low PAPR and Robustness to Phase Noise**:* OFDM has attracted substantial interests because it offers a powerful and practical means to mitigate the effects of ISI in high-throughput MIMO transmissions [58]. However, the DFT operation based modulation at the transmitter disperses each sub-carrier's modulated signal across the entire DFT-block and hence erodes the single-RF benefits of SM-MIMO [87], whilst simultaneously resulting in a high PAPR. By contrast, SC-SM is capable of retaining all the benefits of SM, whilst exhibiting a lower PAPR than its OFDM-based counterpart [66], [71], [87]. As a result, the performance of SM is less affected by the transmitter's power amplifier nonlinearities. A further benefit of SC-SM is its higher robustness both to the frequency offset and to the phase noise, than that of the OFDM scheme, owing to its inherent SC structure.

As an example, we assume that the number of TA is $N_t = 2$, the throughput is $m_{\mathrm{SM}} = 5$ bpcu. The data block size is $K = 256$ and the oversampling factor is set to $\beta = 4$ for PAPR calculation as pulse shaping is considered. In Fig. 10, we present the transmit signal generation and PAPR calculation process of SC-SM and OFDM-SM schemes. The detailed signal generation processes of SC-SM and OFDM-SM are similar to that in Fig. 4, except that a pulse shaping unit is added in SC-SM scheme for practical signal transmission.

Based on the transmit signal model of Fig. 10, the corresponding complementary cumulative distribution functions (CCDFs) of the PAPR of both SC-SM and OFDM-SM systems are shown in Fig. 11. For the sake of simplicity, we only give the CCDF result of the PAPR for the signal vector transmitted over TA 1, since the CCDF result recorded at TA 2 is similar to that of TA 1. The CCDF explicitly shows the probability of having a PAPR, which is higher than a certain PAPR threshold of PAPR_0, namely that we have $\Pr\{\mathrm{PAPR} > \mathrm{PAPR}_0\}$. To evaluate the effects of pulse shaping on SC-SM, we convolve each transmitted symbol waveform with a raised-cosine filter having the roll-off factor α.

As observed in Fig. 11, in the absence of pulse shaping, the PAPR of the SC-SM scheme is about 8.5 dB lower

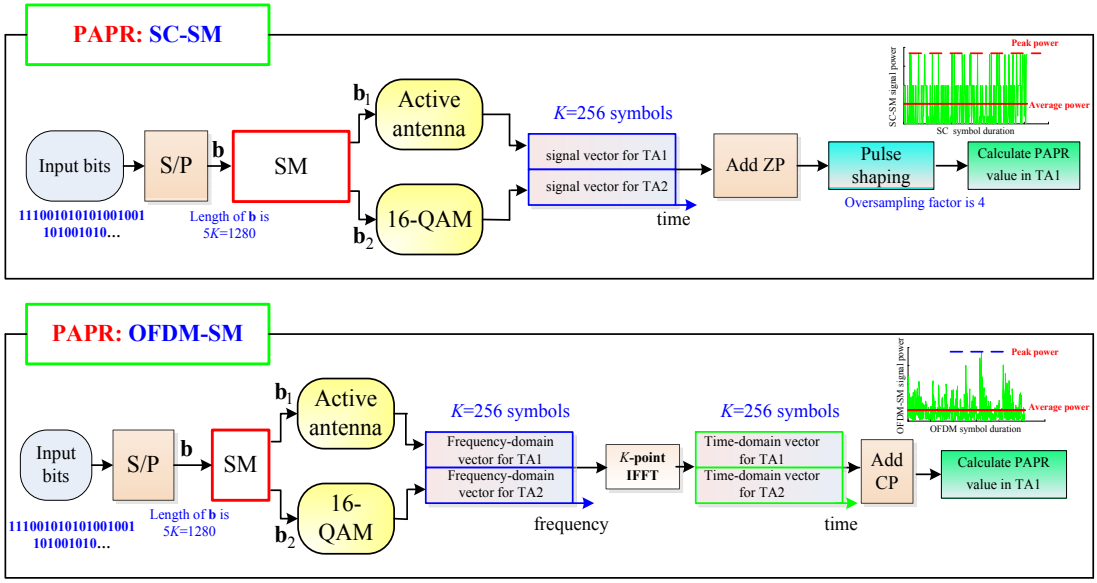

Fig. 10. The example of PAPR calculations for SC-SM and OFDM-SM schemes with $N_t = 2$, $m_{\mathrm{SM}} = 5$ bits/channel-use. We use 4 times oversampling to calculate PAPR for each block when pulse shaping is considered.

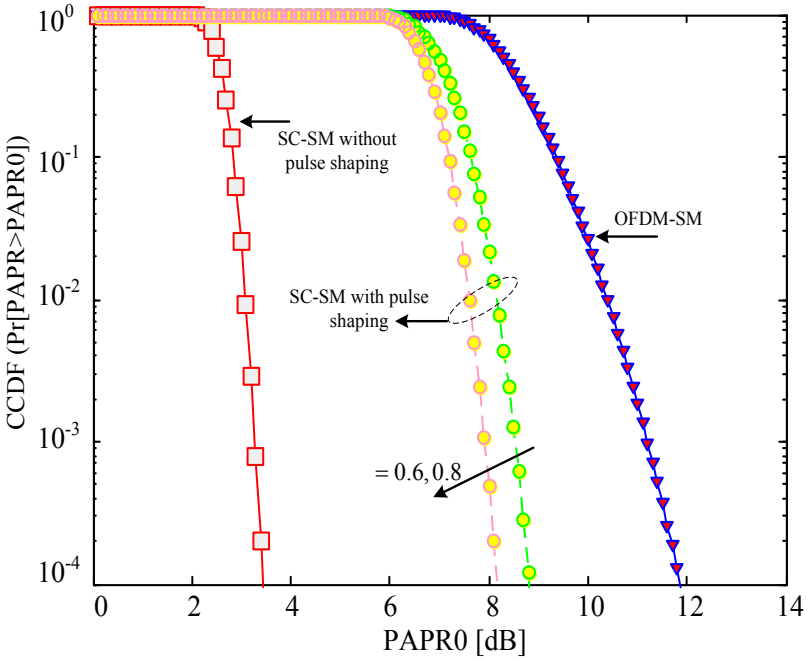

Fig. 11. Comparison of CCDF of PAPR for the SC-SM and the OFDM-SM systems having $N_t = 2$, $K = 256$, $m_{\mathrm{SM}} = 5$ bpcu and operating with 16-QAM constellation. For the SC-SM with pulse shaping in the classic signal domain, the roll-off factor of the raised-cosine pulse filter is $\alpha = 0.6$ and 0.8.

than that of the SC-OFDM scheme at a CCDF of 10^{-3}. As a further metric, the PAPR of the transmitted SC-SM signals only has a 1% probability of being above 3.5 dB. Fig. 11 also shows that in conjunction with the raised-cosine filter, the PAPR increases for the SC-SM schemes, but it still remains better than that of OFDM-SM. It is observed in Fig. 11 that the performance can be improved by using a larger value of the roll-off factor α at the cost of an increased out-of-band radiation [82]. This implies that there is a tradeoff between the attainable PAPR and the out-of-band radiation imposed.

In Fig. 11, the effects of antenna switching in SM are not considered in the design of the pulse shaping filter. As shown in [117], a high roll-off factor is necessary for conventional raised-cosine filter to ensure that the transmit power is concentrated within a short time period so as to enable a single RF chain in SM. Hence, two large values of α are utilized in the PAPR comparison of Fig. 11, such as $\alpha = 0.6$ and 0.8. The design of time-limited waveforms for single-RF based SC-SM scheme is still a challenge, which

will be further discussed in Section V-A.

*4) **High Throughput and High Energy Efficiency**:* As a new three-dimensional (3-D) hybrid modulation scheme, SM exploits the indices of the TAs as an additional dimension invoked for transmitting information, apart from the classic two-dimensional (2-D) APM [82]. SC-SM also adopts this principle and hence achieves a higher throughput than that of the single-antenna and the STBC-MIMO systems. In dispersive channels this gain can be further exploited by using the STdM-like schemes of [79], which relies on the index of the resolvable multipath links as a means of conveying additional source information. Since SM can be realized by using a single RF front-end, the high-cost power amplifier, which is typically responsible for the vast majority of power dissipation at the transmitter, can be reduced. Specifically, recent results based on a realistic power consumption model have shown that a SM-aided base station (BS) has a considerable power consumption gain compared to the multi-RF chain assisted MIMO arrangements (up to 67% more energy efficient in the context of $N_t = 4$) [97]. This energy benefit may also be retained by the SC-SM systems.

*5) **Flexible Design**:* As shown in Fig. 2, due to the single-TA transmission mode, the minimum number of RAs required for efficient detection can be set to one, regardless of how many TA there are. Hence, SC-SM can be flexibly configured for diverse TA and RA configurations, especially for the challenging scenario of asymmetric/unbalanced MIMO systems. As a further advance, SC-SM can be jointly designed in combination with the classic VBLAST and the STBC schemes for striking a flexible tradeoff among the attainable transmit rate, the diversity gain and the cost, which retains the key advantages of SM, while activating multiple TAs [75], [98]. Furthermore, SC-SM can be employed for exploiting the potential multipath diversity or the resolvable multipath-component-based multiplexing gain available in dispersive channels, i.e., the ZP-aided SC-SM scheme of [71] and the STdM scheme of [79]. Additionally, in SC-SM, the prefix vector can be flexibly selected according to the practical system requirements.

B. Some Tradeoffs and Disadvantages

1) Throughput, Diversity, Detection Complexity and RF Cost Tradeoff: In contrast to V-BLAST which is capable of achieving a high multiplexing gain, the family of SC-SM schemes may offer only a logarithmic (rather than a linear) increase of the throughput with the number of TA N_t or the number of TA combinations. This may limit SC-SM for achieving very high spectral efficiencies. Moreover, the conventional SC-SM schemes only achieve receiver diversity and multipath diversity, but no transmit diversity. In conventional narrowband SM scheme, this impediment can be circumvented by employing open-loop as well as closed-loop transmit symbol design techniques [16]. However, these techniques may be not directly suitable for SC-SM systems. Indeed, the degree of freedom in a MIMO system can be allocated by different ways to achieve different tradeoff among different conflicting performance factors. As a new MIMO scheme, SC-SM exploits this degree of freedom to reduce the number of transmit RF chains and the detection complexity, at certain losses of diversity and multiplexing gains.

2) Overhead of Channel Estimation: The coherent detection of the SC-SM scheme in Fig. 2 requires that CSI is available at the receiver. However, it is challenging to acquire accurate CSI of all MIMO channels. The peculiar transmit encoding of SC-SM based over a limited number of RF chains may introduce an additional training overhead, since the CSI of the MIMO subchannels may not be estimated simultaneously.

3) Antenna Array Design: Compared to the conventional full-RF based MIMO schemes, the configuration and deployment of the TA arrays for the single-RF based SC-SM pose some design challenges, because it requires fast TA switching and low spatial correlation between TAs. Due to the unique encoding principle of SC-SM, the active TA index used to convey information may be changed symbol-by-symbol, hence a high-speed RF switching is required. Moreover, SC-SM requires sufficiently low correlation among the channels of the spatial streams for yielding adequate BER performance. Hence, the channel correlation and mutual coupling effects should be carefully considered in the TA array design and implementation for SC-SM based systems.

These above-mentioned advantages and disadvantages indicate that the SC-SM scheme appears to be an attractive low-complexity low-cost option for the emerging family of LS-MIMO systems. Recently, many promising preliminary solutions have been developed to circumvent the above-mentioned disadvantages, which succeeded in improving the tradeoff among the conflicting factor associated with the design of SC-SM systems, such as the computational complexity imposed, the attainable BER, the achievable throughput, the RF cost and the pilot overhead, just to name a few. For example, the SC-GSM scheme may be invoked for improving the throughput, and the STBC scheme can be amalgamated with SC-SM for the sake of increasing the transmit diversity order, while differential SC-SM schemes can be developed for reducing or eliminating the pilot overhead. More related discussions will be provided in Section V. In the next Section, we will provide an up-to-date review of the application of SC-SM in LS-MIMO scenarios.

IV. SC-SM for Multiuser LS-MIMO Systems

The observations and advantages described above have recently sparked off a flurry of research activities aimed at understanding the system design, the signal processing and the detector concepts of SC-SM for conceived multiuser (MU) LS-MIMO systems, as shown in Table VI. In this section, we first review and discuss the SC-based transmission research in the context of LS-MIMO design and then focus our attention on the recent SC-SM schemes proposed for the LS-MIMO transmissions.

TABLE VI
MAJOR CONTRIBUTIONS ON SC-SM AND ITS LARGE-SCALE MIMO DEVELOPMENTS.

Year	Author(s)	Contribution
2008	Mesleh *et al.* [16]	The general bits-to-symbol mapping model of SM was proposed.
2011	Ngo *et al.* [80]	The philosophy of SFSK was proposed, which is a frequency-domain extension of SM for dispersive channels.
	Zhou *et al.* [66]	The concept of SC-SM was proposed for dispersive channels and various linear and nonlinear FDE methods were investigated.
2012	Som and Chockalingam [70]	A diversity analysis framework was proposed for the CP-aided SC-SM.
2013	Rajashekar *et al.* [71]	A ZP-aided SC-SM system was proposed, which is capable of offering full multipath diversity by employing a low-complexity PIC-R-SIC detector.
2014	Narayanan *et al.* [100]	A single-cell downlink broadcast MU SM framework was investigated.
	Humadi *et al.* [101]	A new SM-based transmitter was proposed for large-scale MU downlink transmission systems, where can be viewed an extension of the RSM scheme for MU transmissions.
	Narasimhan *et al.* [105]	The superiority of the large-scale SC-SM over the conventional LS-MIMO was investigated and two low-complexity MU detectors were proposed for uplink transmissions.
	Wang *et al.* [112]	The sparsity and the prior probability distribution of the transmit signal were exploited in the detector design of large-scale CP-aided SC-SM uplink transmission systems.
	Sugiura and Hanzo [87]	An MMSE based low-complexity soft-decision FDE algorithm was proposed for the broadband CP-aided SC-SM systems.
2015	Narasimhan *et al.* [78]	A generalized SC-SM, termed as SC-GSM, was proposed for the LS-MIMO uplink transmission systems, which is capable of striking a trade-off among the transmit rate, the RF cost and the detection complexity.
	Zheng *et al.* [79]	An STdM scheme was proposed for frequency selective fading channels, where the channel time-slot index was employed for conveying additional information.
	Xiao *et al.* [88]	An attractive LSS detector was proposed for the ZP-aided SC-SM, which can efficiently work in the rank-deficient LS-MIMO channels.
	Wang *et al.* [113]	The effects of the low-resolution analog-to-digital convertors (ADCs) were investigated in large-scale CP-aided SC-SM uplink transmissions.

A. SC-based Transmission for LS-MIMO Systems

Again, in the design of LS-MIMO systems, most of the existing contributions rely on the assumption of flat fading channels. One of the reasons for this assumption is that there is some evidence that ISI can be treated as additional thermal noise [10], [65]. However, this assumption has a limited applicability for practical transmissions over dispersive channels, when only a limited number of TAs is available. For the sake of combating the effects of ISI introduced by propagation over frequency-selective fading channels, OFDM is an attractive technique, since it facilities single-tap based equalization. However, it suffers from a high PAPR, as shown in Section III.

For these reasons, various LS-MIMO designs have been investigated in the context of energy-efficient SC or SC-like schemes [12], [63]–[65]. More specifically, in [13], a new soft-output data detector was proposed for uplink transmission by employing SC frequency division multiple access (SC-FDMA)-based LS-MIMO systems. In [13] some practical implementations were conceived for the scenario where all users are equipped with a single antenna. Specifically, the complexity issues of data detection were addressed and a low-complexity soft MMSE-based detector was proposed in [13]. In particular, the inherent matrix inversion of the MMSE algorithm was approximated by a low-complexity Neumann series expansion. It was shown that their proposed method imposes a complexity order of $\mathcal{O}(U^2)$, which is lower than the complexity order of $\mathcal{O}(U^3)$ imposed by the conventional MMSE-based detector, where U is the number of users. However, this approximate method may result in a degradation of BER performance.

In [63] the authors proposed a novel SC-based LS-MIMO scheme for frequency-selective multiuser Gaussian broadcast channels, where efficient downlink precoding was invoked. This transmit precoder (TPC) design is based on the assumption that the number of TAs N_{tot} at the BS is substantially higher than the number of users U ($N_{tot} >> U$). Hence the channel hardening effect can be exploited to design the TPC matrix and the resultant TPC matrix is the linear weighted channel matrix (matched filter), instead of the inversion of the channel matrix. The extent of channel hardening can be viewed a measure of channel orthogonality, as discussed in [7]–[12]. It was shown [63] that the proposed SC scheme achieved a near-optimal sum-rate, with the aid of a low-complexity equalization-free receiver.

More recently, in [64], the symbol-error rates (SERs) of the MF and MMSE detectors were investigated in the context of large-scale multiple-input single-output (MISO) systems both for a negative-exponentially decaying CIR model as well as for the typical urban channel model [99]. It was found [64] that the MMSE based detector performs better than the MF receiver. In [65], the authors investigated the ML equalization of the SC-based LS-MIMO

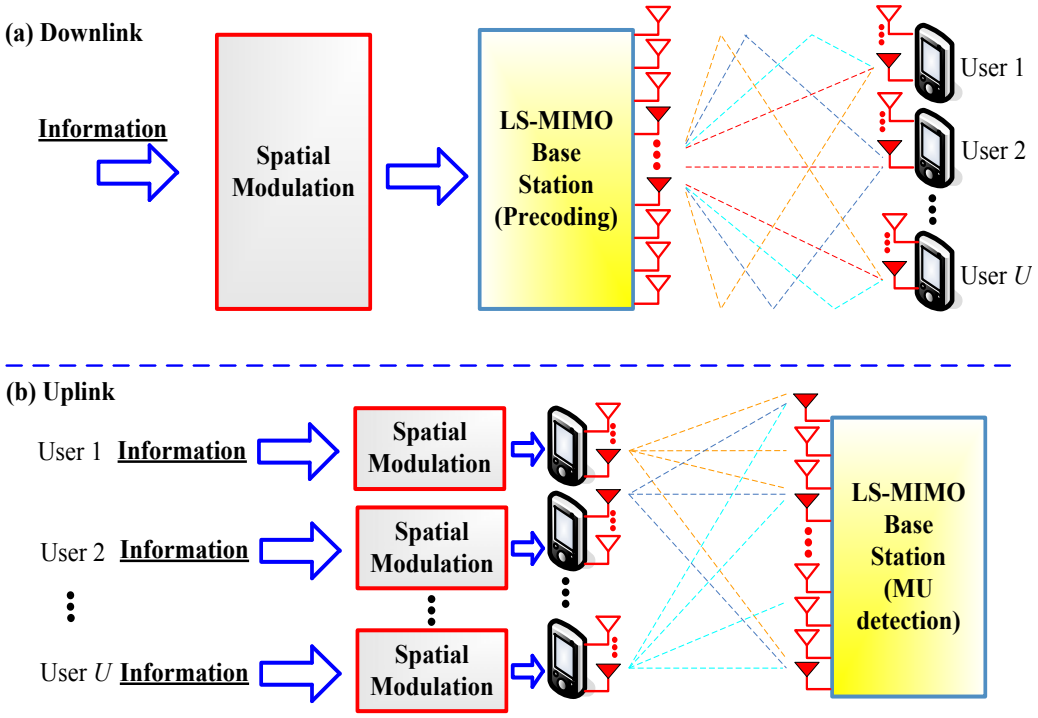

Fig. 12. The design framework for large-scale SC-SM based MU transmission. (a) The general downlink system model. (b) The general uplink system model.

uplink for transmission over a Rician fading channel, in order to mitigate the ISI generated by the combination of the signals received from different antennas through a low-complexity MF. Moreover, by using this novel design, the MU-interference (MUI) caused by the line-of-sight (LOS) components, which may lead to an error-floor in the high SNR region for the conventional single-tap equalizer of [64], can be effectively mitigated.

Note that although the above-mentioned research shows that the SC-based transmission constitutes a promising design alterative for LS-MIMO transmissions, most of the existing research has been based on the assumption that $N_{tot} >> U$ is satisfied and that all users are equipped with a single antenna. The existing solutions may be further improved in order to meet the demand for high-throughput transmissions, in which all the users are equipped with multiple antennas and the number of users U is large. In this case, future SC-based MIMO transmission technique should be designed to satisfy a diverse range of practical requirements and to strike an attractive tradeoff amongst the RF cost, the detection complexity and the BER performance. As it will be shown in the following two subsections, SC-SM can indeed be further developed for designing LS-MIMO systems to achieve these benefits both in downlink and uplink transmissions.

B. SC-SM Large-Scale MIMO Designs for Downlink Transmission

Owing to the compelling advantages of the SC-SM scheme discussed in Section III, recently it has been proposed for the MU LS-MIMO downlink, where the base station may be equipped with hundreds of TAs but only a few RF chains, while each user's receiver can be equipped with either a single or multiple antennas yet relying on a single RF chain. The general downlink model of the multiuser SM based LS-MIMO system is shown in Fig. 12 (a). One of the key design challenges of this architecture is to construct a beneficial TPC for mitigating the MUI.

To this end, in [100] a single-cell downlink MU SM broadcast framework was investigated, which has N_{tot} TAs at the base station and U active users, while each user is equipped with a single RA. In the proposed scheme, the N_{tot} TAs are split into U subsets each associated with N_d TAs and each subset is then allocated to a specific active user. These TA-subsets are then used for an SM-based transmission. Since there is a total of U TA subsets and only a single TA is active in each subset, the number of RF chains required is equal to U. In [100], the SM-based data vector was preprocessed by using a carefully designed TPC for mitigating the MUI, while simultaneously retaining the benefits of SM. As shown in [100], the classic ZF and MMSE TPCs derived for conventional MU MIMO systems are not suitable for SC-SM based MU downlink systems. This is because SM enables data decoding by exploiting the differences among the CIRs of the transmit-to-receive wireless links, but these TPCs may eliminate the channel matrix and hence jeopardize the bits carried by the TA indices. The TPC designed in [100] has considered this effect, which is capable of eliminating of MUI and retaining the CIR differences. The resultant TPC depends on the MU channel matrix $\mathbf{H}_{\text{MU}}$ and can be expressed as $(\mathbf{H}_{\text{MU}})^{-1} diag(\mathbf{H}_{\text{MU}})$, where $diag(\cdot)$ denotes the diagonal

TABLE VII
MAJOR CONTRIBUTIONS ON SC-SM AND ITS LARGE-SCALE MIMO DEVELOPMENTS.

Literature	**Prefix scheme**	**Transmission type**	**Channel coding**	**Channel model**	**RF required**	**CSI estimation**	**Receiver design**
Narayanan *et al.* [100]	N. A.	MU downlink, SM-MIMO	N. A.	Flat-fading	User: 1 BS: U	Perfect CSI	Single-user ML detector
Humadi *et al.* [101]	N. A.	MU downlink, SM-MIMO	N. A.	Flat-fading Flat-fading	User: 1, BS:$N_{\rm tot}$	Perfect CSI	ML detector
Narasimhan *et al.* [105]	N. A.	MU uplink, SM-MIMO	N. A.	Flat-fading	User: 1, BS:$N_{\rm tot}$	Perfect CSI	MP and local search detectors
Wang *et al.* [112]	CP	MU uplink, SM-MIMO	N. A.	Frequency selective channel	User: 1, BS:$N_{\rm tot}$	Least square estimation	Low-complexity generalized MP detector
Sugiura and Hanzo [87]	CP	Point-to-Point, SM-MIMO	Convolutional code	Frequency selective channel	Transmitter: 1	Perfect CSI	Soft MMSE detector and TEQ
Narasimhan *et al.* [78]	CP	MU uplink, GSM-MIMO	N. A.	Flat-fading and frequency selective channel	User:1$\sim$(N_u–1), BS:$N_{\rm tot}$	Perfect CSI, MMSE-based estimation	Two low-complexity MP detectors
Zheng *et al.* [79]	N. A.	Point-to-Point, SM-MIMO	N. A.	Frequency selective channel	Transmitter: 1	Perfect CSI	ML detector
Xiao *et al.* [88]	ZP	Point-to-Point, GSM-MIMO	N. A.	Frequency selective channel	Transmitter: 1$\sim$(N_t–1)	Perfect CSI	LSS detector
Garcia *et al.* [107]	N. A.	MU uplink SM-MIMO	N. A.	Flat Fading	User: 1, BS: $N_{\rm tot}$	Perfect CSI, MMSE estimation	Low complexity CS detector
Wang *et al.* [113]	CP	MU uplink, SM-MIMO	N. A.	Frequency selective channel	User: 1, BS:$N_{\rm tot}$	Least square estimation	Factor graph and MP-based detectors
Yu *et al.* [114]	N. A.	Point-to-Point, GSSK-MIMO	N. A.	Flat-fading	Transmitter: 1$\sim$(N_t–1)	Perfect CSI	Low-complexity CS detector
Liu *et al.* [115]	N. A.	Point-to-Point, GSM-MIMO	N. A.	Flat-fading	Transmitter: 1$\sim$(N_t–1)	Perfect CSI	Low-complexity CS detector
Peng *et al.* [116]	N. A.	Point-to-Point, GSSK-MIMO	N. A.	Flat-fading	Transmitter: 1$\sim$(N_t–1)	Perfect CSI	Sparse K-best detector

U: the number of users.
$N_{\rm tot}$: the number of antennas at BS for the MU transmission.
$N_{\rm u}$: the number of antennas at each user for the MU transmission.
N_t: the number of antennas at transmitter for the point-to-point transmission.

matrix operator.

The simulation results in [100] shows that their proposed scheme is capable of providing the same BER performance as that of the single-user SM transmission, i.e., interference-free. To avoid CSI estimation, an interference-aware detector was also proposed in [100]. Unlike the conventional MIMO-aided MU downlink systems, [100] shows that the direct multi-user detection is not preferred for SC-SM based MU systems. An alternative method is their proposed TPC scheme with single-user detection.

Relying on a novel approach, in [101] the authors proposed a new SM-based transmitter for MU LS-MIMO systems, where the index of the active RA of each user was exploited to convey extra useful information. This scheme can be viewed as an extension of the point-to-point receiver-side SM (RSM) concept of [102]–[104] to MU scenarios. To be specific, in RSM, a particular subset of receive antennas is activated and the specific activated pattern itself conveys useful but implicit information [102]–[104]. In RSM, the classic ZF or MMSE-based TPC schemes can be used for ensuring that no energy leaks into the inactive RA patterns. Based on a similar TPC design principle to that of RSM, a pair of novel methods, termed as subchannel selection and zero-padding, were proposed in [101] for implementing this new SM-based transmitter in the context of MU LS-MIMO downlink systems, where the ZF-based TPC design criterion was used. Moreover, asymptotically tight upper bounds were derived for the average bit error probability (ABEP) of these methods and the simulation results validated that the zero-padding

method is more robust to the MUI [101].

Table VII shows the comparisons of a range of potential SC-SM designs at a glance. We can see that the existing SM-based LS-MIMO downlink transmission schemes have been focused on the TPC designs conceived only for narrow-band scenarios. How to extend these TPCs to broadband transmission is hence an important open issue for future research. A range of open design issues shown in Table VII will be discussed in more detail in Section V.

C. SC-SM Large-Scale MIMO Designs for Uplink Transmission

More recently, SC-SM has also been developed for the uplink of multi-access scenarios and the general system model of the associated uplink SC-SM LS-MIMO system is shown in Fig. 12 (b). Compared to the downlink transmission, the key technological issue in Fig. 12 (b) becomes the design of low-complexity near-optimal detectors for the high-dimensional detection problems faced by the BS equipped with a large number of RAs.

To this end, in [105] the authors proposed a pair of low-complexity detection algorithms for SC-SM based LS-MIMO schemes operating in frequency flat-fading channels, supported by the graph-based message passing (MP) algorithm and the lattice-based local search concepts, respectively. Note that the graph-based MP algorithm is an attractive low-complexity near-optimal approach conceived for large search spaces [108], which has been used for the decoding of turbo codes [109], the detection of MIMO signals [110] as well as for data clustering [111]. The basic idea of the graph-based MP is to graphically represent the factorization of a function and to compute marginals by passing messages over the edges of the graph [108]. The evolved version of the algorithm is mainly dependent on the associated graph structure and on the specific message passing method utilized. In [105], the MU SC-SM LS-MIMO system is represented as a factor graph, where the received symbols were viewed as the observation nodes, while the transmit symbols were viewed as the variable nodes. The messages passed between variable nodes and observation nodes in the factor graph are approximated by a Gaussian distribution, which will be detailed both in the example of Section IV-D and in Fig. 13.

Moreover, in [105] the relationship of the large-scale SC-SM and of the conventional LS-MIMO arrangement was investigated and the numerical results demonstrated that the SC-SM schemes are capable of providing beneficial system performance improvements over the conventional identical-throughput MIMO schemes. For example, SM uplink associated with $N_u = 4$ TAs/user and 4-QAM provides an SNR gain of about 4-5 dB over the conventional LS-MIMO uplink having $N_u = 1$ TA/user and 16-QAM at BER=10^{-3} for 16 users, 128 BS antennas for a throughput of 4 bits/channel-use/user.

The investigations of [105] were further extended in [78], where the generalized SM — GSM concept was considered for the sake of achieving increased-rate data transmission. Furthermore, the authors of [78] provided a closed-form ABEP upper bound expression based on the conventional union-bound method and developed a pair of extensions for the graph-based MP detector designed for SC-GSM signal detection operating in frequency flat-fading channels. It was shown in [78] that the proposed detectors exhibit a considerably reduced complexity, while providing a near-optimal BER performance.

Moreover, the GSM-based system model of [78] was further developed for frequency-selective fading channels. In order to directly use the MP-based detector designed for the flat-fading case, it was combined with a CP-based SC technique for conceiving an equivalent system model. The numerical results demonstrated [78] that the GSM scheme associated with 4 TAs/user, 4-QAM and 2 RF chains provides an SNR gain of about 12 dB over the conventional LS-MIMO having one TA/user and 64-QAM at BER=10^{-3} for 16 users, 128 BS antennas, a throughput of 4 bits/channel-use/user, and a CIR length of $L = 3$. Moreover, it was found that [78] the proposed MP-based detectors are capable of improving the attainable BER performance, despite their reduced complexity, when compared to the classic MMSE detector.

In [112], the MP detector of [105] was further developed for employment in CP-aided SC-SM, where both the sparsity and the probability distribution of the transmit signals were exploited for reducing the MU detection complexity. As shown in [112] the most complex operation required for the proposed detector is constituted by parallelized matrix-vector multiplications, which can be readily implemented in practice. In [112] the un-coded BER of the proposed MP-based detector was evaluated by applying the state evolution (SE) method, which is widely used to predict the performance of MP-like algorithms. Simulation results in [112] showed that the proposed MP algorithm is capable of achieving the near-ML performance. Moreover, an energy-efficient SC-SM scheme was proposed [112], which adjusts the transmit parameters for optimizing the energy consumption at a predefined target BER.

Based on the system model of [112], in [113] the authors investigated the MU detection issues in more practical scenarios, where the BS was equipped with low-resolution analog-to-digital convertors (ADCs), only impose a low circuit-power consumption on the LS-MIMO system. In [113], the classic least-square channel estimator was invoked and a novel low-complexity MP de-quantization detector was proposed, relying on the clustered factor graph method and the central limit theorem. The simulation results of [113] have shown that the proposed detector outperforms the existing linear detectors and can efficiently operate under realistic LS-MIMO channel conditions, when the antennas are insufficiently far apart to avoid correlated fading.

In [107] a low complexity detector was designed for the uplink of LS-MIMO systems using SC-SM, which was based on a CS approach. It was shown that the signal structure of SM in the multiple access channel can be

exploited for providing additional information and for improving the performance of the CS algorithms. The simple SC-SM detector was shown to offer a substantially improved energy-efficiency compared both to classical MIMO detectors and to conventional SM detection approaches.

D. Uplink SC-SM LS-MIMO System Example and Performance Results

In Fig. 13, we provide an example for an uplink SC-SM LS-MIMO transmission scheme, which has $N_{tot} = 64$ antennas at the BS and U active users. Each user is equipped with $N_u = 4$ TAs. For all users, we assume that the length of transmit frame is $K = 128$ and QPSK modulation ($M_{\rm SM} = 4$) is employed for each TA. Based on the SC-SM framework in Fig. 2 and Table I, it is easy to show that the throughput of this scheme is $m_{\rm SM} = \log_2(N_u M_{\rm SM}) = \log_2(4 \times 4) = 4$ bits/channel-use/user, in which $\log_2(N_u) = 2$ TA-bits are conveyed by TA indices and another $\log_2(M_{\rm SM}) = 2$ APM-bits are conveyed by the APM symbols. Moreover, the following SM mapper is used: all possible pairs of TA-bit combinations $\{[0\ 0], [0\ 1], [1\ 0], [1\ 1]\}$ are mapped to the TA indices of $\{1, 2, 3, 4\}$. Explicitly, TA 1 is activated when the input TA-bits are [0 0], TA 2 is activated when the input TA-bits are [0 1], TA 3 is activated when the input TA-bits are [1 0], and TA 4 is activated when the input TA-bits are [1 1]. Similarly, all possible APM-bit combinations $\{[0\ 0], [0\ 1], [1\ 1], [1\ 0]\}$ are one-to-one mapped to the classic QPSK constellation points $\{+1, +j, -1, -j\}$, i.e. [0 0] is mapped to the QPSK signal "+1" and [0 1] is mapped to QPSK signal "+j". Based on **Algorithm 1** and [78], Fig. 13 shows the detailed operations in an SC-SM based MU transmitter as well as the corresponding MP algorithm based receiver for this 4 bits/channel-use/user system.

As shown in Fig. 13, 4 bits are transmitted in each channel use for each user, hence the information bit stream is divided into multiple 4-bit vectors, each of which is further divided into 2 TA-bits and 2 APM-bits. Then, based on the SM mapping rule described above, the two TA-bits are used to activate an unique TA for transmission, while the two APM-bits are mapped to a QPSK symbol. For example, in Fig. 13, the first bit vector $\mathbf{b}_1(1) = [1\ 1\ 0\ 1]$ of user 1 is divided into the TA-bit vector [1 1] and the APM-bit vector [0 1], which are mapped to TA 4 and the QPSK symbol $+j$, respectively. According to Eq. (1), the resultant SM symbol based on $\mathbf{b}_1(1)$ can be formulated as $\mathbf{x}_1(1) = [0\ 0\ 0\ \ +j]^T \in \mathbb{C}^{N_t \times 1}$. Fig. 13 shows the detailed transmitted frame generation process based on **Algorithm 1** for each user and provides examples for TA activation and QPSK signal transmission for the first symbol $\mathbf{x}_i(1), i \in \{1, \cdots, 16\}$ of each user. An earlier example on the SC-SM signal generation process can also be found in Section II-B.

Recently, a graph-based MP algorithm has been proposed in [78]. To describe its operating principle, we consider the MP detection in the context of flat-fading channels, which can be readily extended to frequency-selective fading scenarios by formulating an equivalent channel model, as shown in [78]. Let $\bar{\mathbf{H}}(k) \in \mathbb{C}^{N_{tot} \times UN_u}$ denote the channel matrix in the kth time slot, whose element $\bar{h}_{i,(u-1)N_u+j}(k)$ denotes the channel gain associated with the link spanning from the jth TA of the uth user to the ith BS RA. The signal received at the BS of the kth time slot is formulated by

$$\begin{aligned} y_i(k) &= \sum_{u=1}^{U} \bar{\mathbf{h}}_{i,[u]}(k)\mathbf{x}_u(k) + n_i(k) \\ &= \underbrace{\bar{\mathbf{h}}_{i,[u]}(k)\mathbf{x}_u(k)}_{\text{user } u} + \underbrace{\sum_{j=1, j\neq u}^{U} \bar{\mathbf{h}}_{i,[j]}(k)\mathbf{x}_j(k)}_{\text{MUI}} + \underbrace{n_i(k)}_{\text{noise}}, \end{aligned} \quad (3)$$

where $\bar{\mathbf{h}}_{i,[u]}(k) \in \mathbb{C}^{1 \times N_u}$ is obtained from the ith row of $\bar{\mathbf{H}}(k)$ and of the $(u-1)N_u + 1$ to the uN_u columns of $\bar{\mathbf{H}}(k)$, with $n_i(k)$ being the noise term. As shown in Eq. (3), to detect the signal transmitted by the uth user, the received signal $y_i(k)$ can be divided into three components: the component with useful information for user u, the MUI component from other users, and the noise component.

Based on Eq. (3), in Fig. 13 the MU SC-SM LS-MIMO system is represented as a factor graph. Observe in Fig. 13 that the received signals $y_i(k), i = 1, \cdots, 64$ can be viewed as the observation nodes, while the transmit symbols $\mathbf{x}_u(k), u = 1, \cdots, 16$ for the kth time slot can be viewed as the variable nodes. The messages passed between variable nodes and observation nodes in the factor graph are approximated by a Gaussian distribution. To be specific, the summation of the MUI and noise term $N_{iu}(k) = \sum_{j=1, j\neq u}^{U} \bar{\mathbf{h}}_{i,[j]}(k)\mathbf{x}_j(k) + n_i(k)$ of Eq. (3) is approximated as a Gaussian random variable with a mean of $\mu_{iu}(k)$ and a variance of $\sigma^2_{iu}(k)$.

In the graph-based MP-based detection, some specific messages are iteratively exchanged between the observation nodes $y_i(k), i = 1, \cdots, 64$ and the variable nodes $\mathbf{x}_u(k), u = 1, \cdots, 16$, in order to achieve improved estimation result. In our example, the specific messages sending from an observation node to a variable node are the scalar variables $\mu_{iu}(k)$ and $\sigma^2_{iu}(k)$, which are the mean and variance of the sum of MUI and noise $N_{iu}(k)$, respectively. The message from variable nodes $\mathbf{x}_u(k)$ to observation nodes $y_i(k)$ is a vector about the a posteriori probability $p^k_{ui}(\mathbf{s})$ of all possible transmitted SM symbols $\mathbf{s}$. Note that there are 16 legitimate SM symbols $\mathbf{s}$ for 4 bits/channel-use/user, which are given at the bottom of Fig. 13, the probability vector of which can be expressed as $\mathbf{p}^k_{ui}(\mathbf{s}) = [p^k_{ui}(\mathbf{s}_1), p^k_{ui}(\mathbf{s}_2), \cdots, p^k_{ui}(\mathbf{s}_{16})]$.

With the knowledge of $\mu_{iu}(k)$ and $\sigma^2_{iu}(k)$, the a posteriori probability $p^k_{ui}(\mathbf{s})$ of all possible transmitted SM symbols $\mathbf{s}_l, l = 1, \cdots, 16$ for the uth user in the kth time slot is given by

$$p^k_{ui}(\mathbf{s}) \propto \prod_{m=1, m\neq i}^{N_{tot}} \exp\left(\frac{-\left| y_i(k) - \mu_{mu}(k) - \bar{\mathbf{h}}_{m,[u]}(k)\mathbf{s}_m \right|^2}{2\sigma^2_{mu}(k)} \right). \quad (4)$$

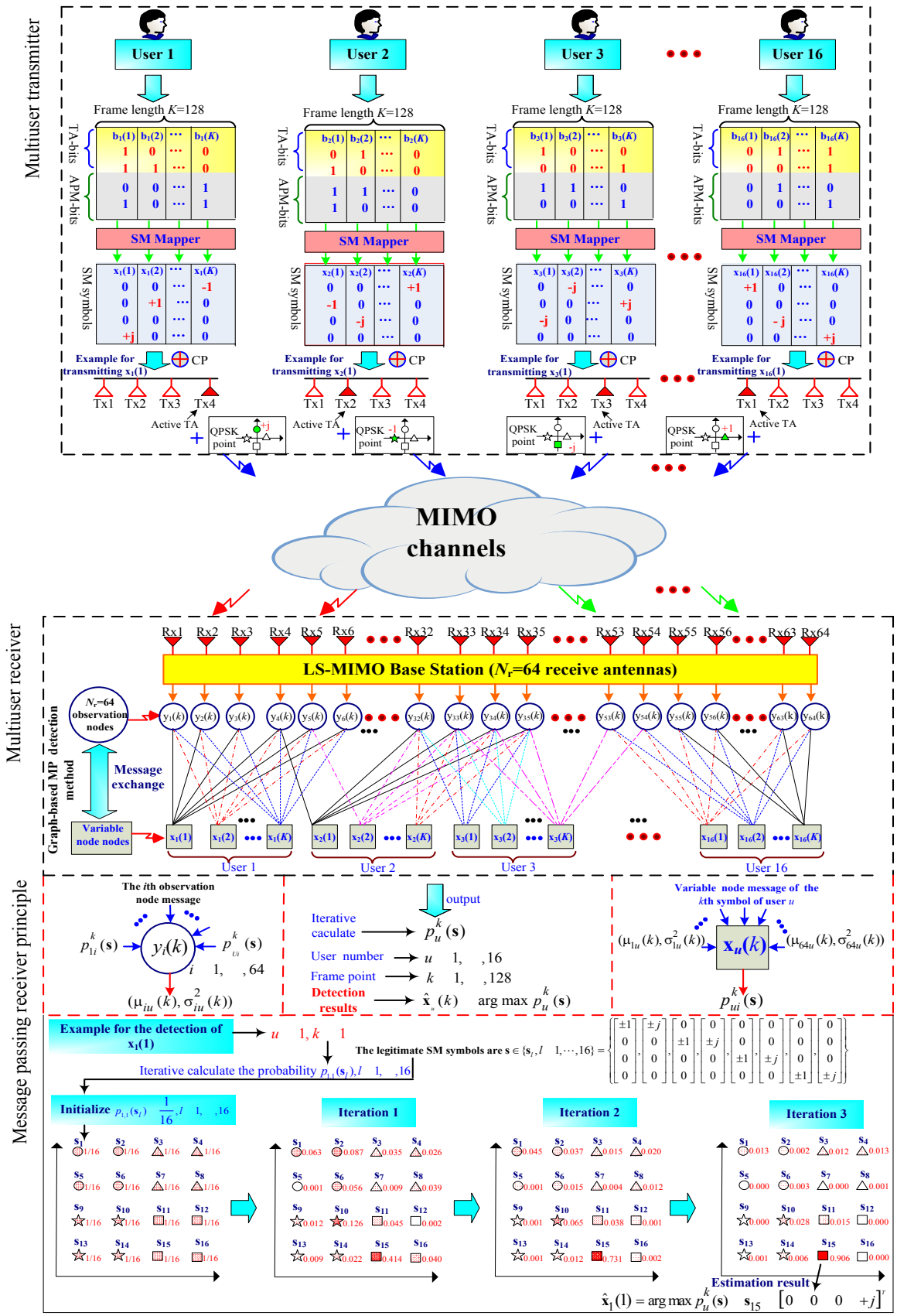

Fig. 13. An example of CP-aided SC-SM LS-MIMO system associated with $U = 16$, $K = 128$, $N_{tot} = 64$, $N_u = 4$ and QPSK modulation, employing the MP-based detector.

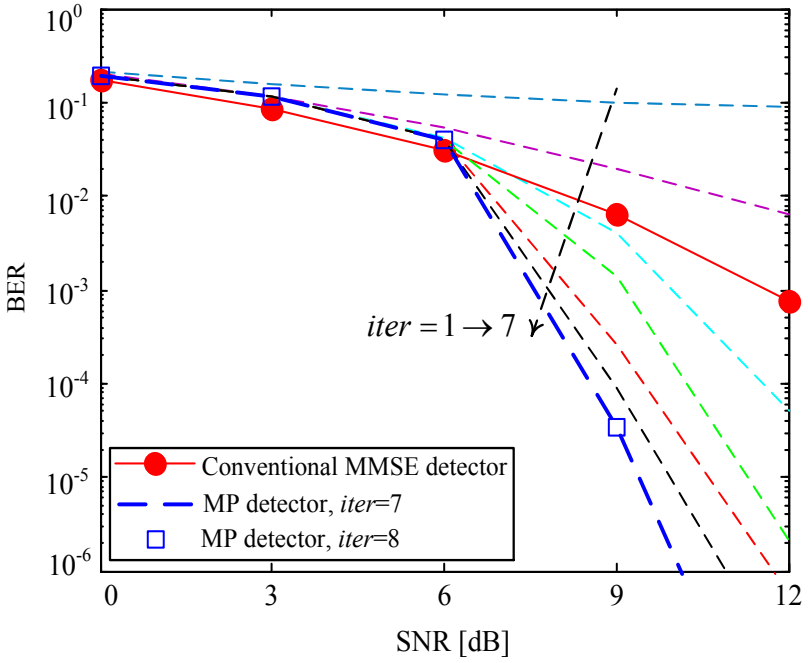

Fig. 14. BER performance of multiuser CP-aided SC-SM LS-MIMO system associated with $U = 16$, $K = 128$, $N_{tot} = 64$, $N_u = 4$ and QPSK modulation for transmission over the EVA model, where the MP-based detector is employed. The iteration number of MP-based detector is $iter = 1 - 8$. Furthermore, the conventional MMSE-based multiuser detector is also consider as benchmarker

Note that the calculation of $p_{ui}^k(\mathbf{s})$ is independent of the observation node $y_i(k)$ itself, hence this message can be viewed as the extrinsic information, which is passed to the observation node $y_i(k)$ as the a posteriori probability for estimation of the massages $\mu_{iu}(k)$ and $\sigma_{iu}^2(k)$ in the next iteration. The message exchanges between these factor nodes are iteratively carried out and the final detection is achieved by the following probability

$$p_u^k(\mathbf{s}) \propto \prod_{i=1}^{N_{tot}} \exp\left(\frac{-\left|y_i(k) - \mu_{iu}(k) - \bar{\mathbf{h}}_{i,[u]}(k)\mathbf{s}\right|^2}{2\sigma_{iu}^2(k)}\right). \quad (5)$$

Compared to the extrinsic information $p_{ui}^k(\mathbf{s})$ in Eq. (4), the final decision metric $p_u^k(\mathbf{s})$ relied on the values of all observation nodes. Finally, the detected SM signal of the uth user in the kth time slot is formulated as:

$$\hat{\mathbf{x}}_u(k) = \arg\max_{\mathbf{s}} p_u^k(\mathbf{s}). \quad (6)$$

Then, $\hat{\mathbf{x}}_u(k)$ is demodulated by the SM demapper to the original data bit sequence.

In Fig. 13, we give a simple example for the detection of $\mathbf{x}_1(1) = [0\ 0\ 0\ \ +j]$ of user 1 by employing the above-mentioned graph-based MP algorithm. According to Eq. (6), the detection of $\mathbf{x}_1(1)$ relies on the probabilities $p_1^1(\mathbf{s}_l)$, $l = 1, \cdots, 16$, calculated by Eq. (5). In the initial stage of message exchange, all of these values are set to be $\frac{1}{16}$. Then, as the number of iterations increases, the MP algorithm begins to acquire these metrics $p_1^1(\mathbf{s}_l)$, $l = 1, \cdots, 16$ by updating the massages of $\mu_{iu}(k)$, $\sigma_{iu}^2(k)$ and $p_{ui}^k(\mathbf{s})$. As shown in Fig. 13, after about 3 iterations, the value of $p_1^1(\mathbf{s}_{15})$ becomes the highest in the set of $p_1^1(\mathbf{s}_l), l = 1, \cdots, 16$. To be specific, it is equal to 0.414 in the first iteration, increases to 0.731 after the second iteration and reaches 0.906 after the third iteration. Based on the example of Fig. 13 and on Eq. (6), it is found that the SM symbol $\mathbf{s}_{15}$ is the final estimation result, which corresponds to the correct detection of $\mathbf{x}_1(1)$.

Based on a similar setup to that seen in Fig. 13 and [78], in Fig. 14 we evaluated the BER performance of a multiuser CP-aided SC-SM LS-MIMO system associated with $U = 16$, $K = 128$, $N_r = 64$, $N_t = 4$ and QPSK modulation for transmission over the EVA model, where the MP-based detector of [78] is employed. The number of iterations (denoted by $iter$) employed by the MP-based detector is 8. Furthermore, the conventional MMSE-based multiuser detector is also considered as a benchmark. As shown in Fig. 14, the MP algorithm has converged after 7 iterations, since the BER performance of $iter = 7$ and $iter = 8$ is almost identical. As expected, the MP-based detector is capable of efficiently detecting the SM symbols in large dimensions, as seen in Fig. 14, which outperformed the conventional MMSE detector by about 5 dB at a BER of 10^{-3} after 8 iterations. Moreover, as shown in [78], in addition to having this BER gain, the MP-based detector exhibits a considerably lower complexity than that of the MMSE-based detector, because it uses a low-complexity iterative message exchange process for avoiding the high-complexity channel inversion of the MMSE scheme. To be specific, the approximate complexity order of the MP-based detector is $\mathcal{O}(N_{tot} K N_u M_{\mathrm{SM}})$, while the complexity order of the MMSE-based detector is $\mathcal{O}(N_{tot}^2 K N_u)$. The MP-based detection exhibits considerable complexity reduction, since we have $N_{tot} >> N_u M_{\mathrm{SM}}$ in LS-MIMO systems.

TABLE VIII

Comparison of SC-SM, SC-GSM, SIMO, and VBLAST based MU LS-MIMO uplink transmission systems.

Scheme	SC-SM LS-MIMO	SC-GSM LS-MIMO	SIMO LS-MIMO	VBLAST LS-MIMO
Throughput (bits/channel-use/user)	$T_{\mathrm{SM}} = \log_2(N_u M_{\mathrm{SM}})$	$T_{\mathrm{GSM}} = \left\lfloor \log_2 \binom{N_u}{N_g} \right\rfloor + N_g \log_2(M_{\mathrm{GSM}})$	$T_{\mathrm{SIMO}} = \log_2(M_{\mathrm{SIMO}})$	$T_{\mathrm{VBLAST}} = N_u \log_2(M_{\mathrm{VBLAST}})$
RF chains/user	1	$N_g (N_g < N_u)$	1	N_u

M_{GSM}: the APM order in SC-GSM scheme.

M_{SIMO}: the APM order in SIMO scheme.

$\lfloor \cdot \rfloor$: the floor operator.

Based on Table VII and our example, we can see that the above-mentioned SC-SM designs for LS-MIMO uplink transmissions are more focused on the MU detector designs for the family of CP-aided SC-SM schemes. By contrast, as shown in Section II, the family of ZP-based SC-SM schemes may be preferred over its CP-based counterpart and further investigations about the ZP-aided SC-SM designs are required. In Table VIII, we compare the throughput and the number of RF chains required for different MU LS-MIMO schemes, where the SC-GSM based MU LS-MIMO is capable of striking a flexible throughput versus RF cost tradeoff. Moreover, in [78], a BER comparison between the MU SC-GSM LS-MIMO and MU SIMO LS-MIMO was presented to study the advantages of SC-SM schemes. It was shown that the MU SC-GSM LS-MIMO outperforms the conventional MU SIMO LS-MIMO by about 10 dB in terms of SNR at the throughput of 6 bits/channel-use/user. Nevertheless, current research results are still preliminary and further investigations are required to identify the benefits of the family of MU SC-SM LS-MIMO schemes over other LS-MIMO schemes.

Furthermore, as discussed in Sections I and III, SM can be realized by using a single RF front-end, hence it has a high power efficiency in realistic BS models. As shown in [97], in flat-fading channels SM has a considerable power consumption gain compared to multi-RF chain aided MIMO arrangements (e.g., STBC and VBLAST). However, in multipath channels, it is more challenging to evaluate the capacity of SC-SM for energy efficiency evaluation. Whether the benefits of energy efficiency observed in narrowband SM are still retained in broadband MU LS-MIMO scenarios requires further justification. More detailed discussions and potential solutions in the uplink and downlink SM-based LS-MIMO systems will be provided in the next Section.

V. Further Design Issues

According to the above-mentioned advantages and based on the initial results, SC-SM may be deemed to be an attractive low-complexity, low-cost design option for the emerging family of LS-MIMO systems, which is still in its infancy. To make the SC-SM based LS-MIMO systems a commercial reality, there are still numerous open issues that have to be studied. Some of these challenges and their potential solutions are shown in Fig. 15 and will be discussed below.

A. High-Speed Antenna Switching

The single-RF chain based design of SC-SM schemes requires an agile RF switch. The basic effects of this switch should be carefully resolved, namely the potential data loss inflicted by the shaping filter and the energy efficiency loss of the power amplifier caused by the isolated pulses transmitted in the time-domain. To combat these limitations while relying on less RF chains than the number of TA elements, in [117] the authors quantified the above-mentioned performance penalty in terms of the bandwidth efficiency reduction and proposed a practical RF chain switching method, which is capable of operating in conjunction with a longer pulse shape than that facilitated by a single-RF aided SM scheme. Moreover, in [118], a novel RF chain was designed for facilitating the smooth changing of the currents on the TAs, which constitutes an efficient alterative for pulse shaping technique. Another potential design is the employment of low-complexity time-domain raised-cosine pulse shaping, which simply over-samples the waveform by a sufficiently high factor and then smoothly transitions between the consecutive symbols. This can be attained, for instance, by reading the pre-stored intermediate values for all legitimate transitions from a look-up table [119]. However, to invoke these techniques in the context of SC-SM based LS-MIMO systems, more detailed investigations are needed.

B. Soft-Input-Soft-Output Detector Design

The signal dimension of SC-SM depends both on the frame length and on the number of antennas, which becomes high in the context of LS-MIMOs. There is a growing literature on how to design both linear and non-linear detectors for conventional LS-MIMO schemes, such as the lattice-based likelihood ascent search (LAS) [120] and the factor-graph based belief propagation algorithms [121]–[123]. However, they may not be directly applicable to the SC-SM based LS-MIMO schemes.

Here explicitly, most of the detectors designed for SC-SM in Section III may only be suitable for small-scale SC-SM systems, which commonly rely on 2-4 antennas at both

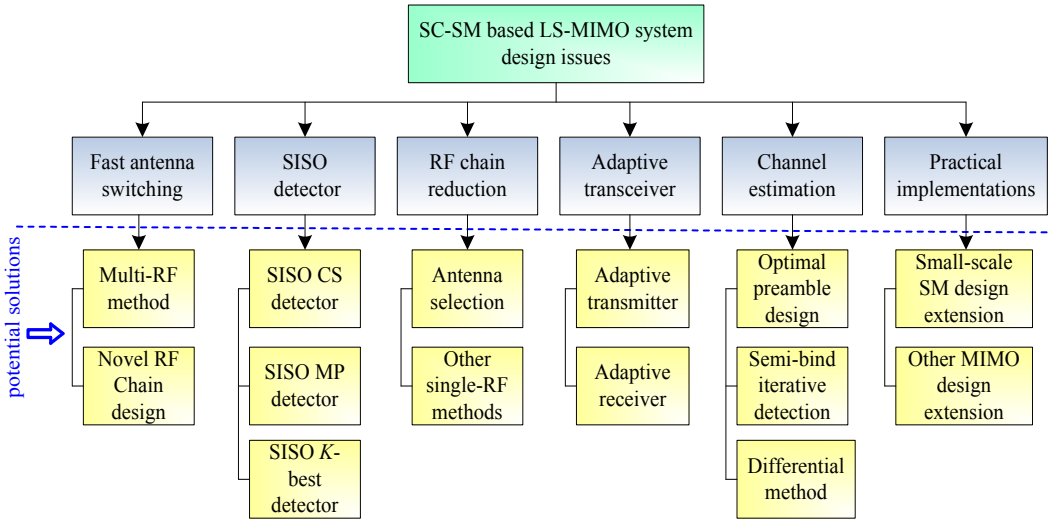

Fig. 15. The future design issues and the related potential solutions for the SC-SM based LS-MIMO.

ends of the wireless link. For large-scale SC-SM uplink transmission, the MP methods were proposed in [105], [112], [113], [124], but they are rely on hard decisions. However, in practice almost all wireless communication systems employ some form of FEC for enhancing the data reliability, which requires soft-input soft-output (SISO) detectors for achieving the highest possible coding gain.

Additionally, for the sake of reducing the computational complexity, most of the existing detectors were proposed for the family of CP-aided SC-SM schemes, where low-complexity single-tap equalization can be used, as shown in Table VII. However, this benefit is achieved under the constraint of $N_t \leq N_r$, which erodes the performance of SM in asymmetric MIMO systems, routinely encountered in downlink transmission. In the future, the SISO detectors designed for high-diversity ZP-aided large-scale SC-SM have to be further investigated.

Since the generalized MP detectors of [105], [112], [113], [124], as well as the CS of [114], [115] and the sparse K-best detector of [116] provide significant detection complexity reductions by exploiting the inherent sparsity of the SC-SM-type signaling regime, these SISO versions may indeed be promising alternatives for SC-SM based LS-MIMO transmissions and they are worth more intensive study.

C. Further RF Chain Reduction

SM may be viewed as a special case of transmit antenna selection (AS). Unlike the AS techniques conceived for the conventional MIMO systems of [125], which rely on the channel quality often quantified in terms of the received signal strength, AS in SM is controlled by the incoming user data stream. SM enjoys the prominent benefit that the number of RF chains required is substantially reduced.

As shown in Section IV and Table VII, several attractive TPC schemes have been proposed for SC-SM based LS-MIMO downlink transmission systems [100], [101]. Although the AS-like SM scheme can reduce certain parts of RF chains, they still require a large number of RF chains at the BS for optimizing the precoder, which may jeopardize the most salient advantages of SC-SM. To further reduce the associated cost, the classic AS technique can be amalgamating the concept of SM for reducing the number of RF chains, without unduly eroding the attainable system performance. Especially, when a large number of antennas are used at the BS, the propagation channel potentially provides much more spatial selectivity, than in small-scale scenarios. In this case, the beneficial system performance gain provided by the carefully designed AS schemes will also become more attractive.

Note that in recent years various AS techniques have been proposed for the family of conventional SM schemes [126]–[132]. However, they have been designed for frequency flat-fading scenarios and hence may not be directly applicable to the more sophisticated SC-SM scheme. One of the key design challenges of AS conceived for SC-SM based LS-MIMO systems is to construct a beneficial AS criterion, while relying both on a low-complexity and on a modest amount of feedback information. Moreover, a range of other RF chain reduction techniques may be combined with the SC-SM technique, in order to further reduce the cost of the hardware as exemplified by the single-RF based time-division multiplexing techniques and by the parasitic antenna method of [133].

D. Practical Implementations

Experimental studies have also been conducted for evaluating the SM-based transceiver in an indoor propagation scenario [56], [57], where the BER performance of small-scale MIMO channels (i.e. the 2×2 and the 4×4 MIMO configurations) operating both in LOS and non-LOS scenarios was investigated. The measured results confirmed that the theoretical gains predicted by the analysis are substantiated by the Monte Carlo simulations [56]. Moreover, it was shown in [57] that the SM-based scheme performs better than the VBLAST and STBC

schemes in the context of the measured channel models considered.

Note that these preliminary results were performed in a controlled laboratory environment in conjunction with a small number of antennas, where the effects of dispersive channels and the impact of the associated hardware impairments have not been considered. On the other hand, for conventional LS-MIMO systems, the authors of [134] has provided some experimental results for SC modulation communicating over measured massive MIMO channels with 128 TAs. It was shown that the effects of ISI have to be carefully considered in conventional LS-MIMO systems, similar to the initial MU SC-SM based LS-MIMO design framework shown in Fig. 13. These observations and investigations may be extended to large-scale MU SC-SM schemes operating in realistic propagation scenarios, so as to verify the related benefits of SC-SM in MU LS-MIMO systems.

E. Adaptive Transceiver Design

Adaptive transceivers play an important role in wireless communication systems, which are capable of dynamically adjusting the transceiver parameters in response to the time-variant channel conditions [135], [136]. Hence they have been extensively studied in the conventional SM context for the sake of improving the achievable BER performance and of reducing the detection complexity [137]–[143], whilst relying on adaptive modulation [137], [138], on constellation optimization [54], [139]–[142], on power allocation [143], [144] as well as on phase rotation techniques [145]–[149]. However, it has not been considered, whether these adaptive techniques can be directly applied to the SC-SM based LS-MIMO systems. Even for the conventional LS-MIMO schemes, only limited initial work has been disseminated on the design of AS methods and on adaptive receivers [150], [151]. Near-capacity adaptive techniques, relying on low complexity and a low feedback requirement, are worth more intensive study.

F. Channel Estimation and Low-Correlation Preamble Sequence Design

A key design challenge in LS-MIMO systems (including SC-SM based LS-MIMO) is how to achieve optimal estimation of the CSI. A common approach to acquire CSI is to send properly designed preambles (or pilot signals) from the transmitter(s) and then estimate the channel impairments in the receiver by correlating the known preambles (locally generated) with the received signals. However, this process is always prone to estimation errors. For small-scale SM, the effects of these errors have been investigated in [41], [42], [152]–[155] and it was shown that SM is more robust to channel estimation errors than VBLAST. However, this advantage of SM has not been investigated in large-scale SC scenarios.

It is noted that optimal channel estimation in general requires the preamble sequences to have zero non-trivial auto- and cross-correlations [156]–[159]. However, the employment of conventional preamble sequences may jeopardize the advantages of SC-SM, since they have not been designed by taking into account the sparse structure of SC-SM symbols. To overcome this impediment, [112] and [113] developed the training sequences by using cyclic right-shifting method for SC-SM based on the MU channel estimation process, which was proposed for uplink LTE transmissions. However, this design may not be suitable for high-rate SC-SM schemes, owing to the associated power efficiency loss and the pilot overhead imposed. In all existing MIMO-oriented pilot sequences, the ternary-like pseudo-random sequences of [160] may be a promising candidate, including the family of SC-SM and SC-GSM schemes, because its spatial-domain sparsity can be flexibly adjusted. Nonetheless, additional work is necessary to make the associated design more practical.

In order to reduce the pilot-overhead, the semi-blind iterative detection technique of [161], the advanced training optimization techniques of [162] and the differentially encoded designs of [163]–[168] may be important future research directions.

VI. Conclusion

In this paper, we reviewed a range of recent research achievements related to SC-SM, which constitutes a new low-complexity low-cost broadband MIMO transmission technique recently proposed. This novel scheme is capable of adopting the low-complexity single-stream based detection, whilst relying on a single RF chain. Moreover, it can be designed for striking a flexible trade-off amongst the range of potentially conflicting system requirements, such as the effective throughput, the diversity gain and the hardware cost, while facilitating communications over dispersive channels. The scheme reviewed here constitutes a promising candidate for LS-MIMO aided MU uplink and downlink design. However, for exploiting its full benefits numerous challenges have to be overcome.

List of Acronyms

ABEP	Average Bit Error Probability
ADCs	Analog-to-Digital Convertors
APM	Amplitude and Phase Modulation
APM-bits	Amplitude and Phase Modulation-bits
AS	Antenna Selection
BER	Bit Error Rate
BS	Base Station
CCDF	Complementary Cumulative Distribution Function
CFO	Carrier Frequency Offset
CIR	Channel Impulse Response
CP	Cyclic Prefix
CS	Compressive Sensing
CSI	Channel State Information
DFT	Discrete Fourier Transform

DFE	Decision-Feedback Equalizer
EVA	Extended Vehicular A Model
FDE	Frequency-Domain Equalization
FEC	Forward Error Correction
FH-CDMA	Frequency Hopping Code Division Multiple Access
GSSK	Generalized Space Shift Keying
GSM	Generalized Spatial Modulation
IBI	Inter-Block Interference
IFFT	Inverse Fast Fourier Transform
KSP	Known Symbol Padding
LAS	Likelihood Ascent Search
LLRs	Log-Likelihood Ratios
LOS	Line of Sight
LSA	Large-Scale Antenna
LS-MIMO	Large-Scale Multiple-Input Multiple-Output
LSS	Low-Complexity Single-Stream
MAC	Multiple Access Channel
MAP	Maximum A Posteriori
MF	Matched Filter
MIMO	Multiple-Input Multiple-Output
ML	Maximum-Likelihood
MMSE	Minimum Mean-Squared Error
MP	Message Passing
MU	Multiuser
MUI	Multiuser-Interference
OFDM	Orthogonal Frequency-Division Multiplexing
PAPR	Peak-to-Average Power Ratio
PIC	Parallel Interference Cancellation
PIC-R-SIC	PIC-based Receiver With SIC
QRD-M	QR Decomposition With M-algorithm
RA	Receive Antenna
RF	Radio Frequency
RSM	Receiver-Side Spatial Modulation
SC	Single-Carrier
SC-FDE	Single-Carrier Systems Using Frequency-Domain Equalization
SC-FDMA	Single-Carrier Frequency Division Multiple Access
SC-SM	Single-Carrier-Based Spatial Modulation
SD	Sphere Decoding
SE	State Evolution
SER	Symbol Error Rate
SFSK	Space Frequency Shift Keying
SIMO	Single-Input Multiple-Output
SISO	Soft-Input Soft-Output
SIC	Successive Interference Cancellation
SM	Spatial Modulation
SNR	Signal-to-Noise Ratio
SSK	Space Shift Keying
STdM	Space and Time-dispersion Modulation
STBC	Space Time Block Code
TA	Transmit Antenna
TA-bits	Transmit Antenna-bits
TDE	Time-Domain Equalizer
TEQ	Turbo Equalizer
TPC	Transmit Precoder
VBLAST	Vertical Bell Labs Layered Space-Time
ZF	Zero Forcing
ZP	Zero Padding

References

[1] J. Mietzner, R. Schober, L. Lampe, W. H. Gerstacker, and P. A. Hoeher, "Multiple-antenna techniques for wireless communications–A comprehensive literature survey," *IEEE Commun. Surveys Tuts.*, vol. 11, no. 2, pp. 87-105, Second Quarter, 2009.

[2] S. Sugiura, S. Chen, and L. Hanzo, "A universal space-time architecture for multiple-antenna aided systems," *IEEE Commun. Surveys Tuts.*, vol. 14, no. 2, pp. 401-420, Second Quarter, 2012.

[3] L. Zheng and D. N. C. Tse, "Diversity and multiplexing: A fundamental tradeoff in multiple-antenna channels," *IEEE Trans. Inf. Theory*, vol. 49, no. 5, pp. 1073-1096, May 2003.

[4] B. Hassibi and B. M. Hochwald, "High-rate codes that are linear in space and time," *IEEE Trans. Inf. Theory*, vol. 48, no. 7, pp. 1804-1824, Jul. 2002.

[5] V. Tarokh, H. Jafarkhani, and A. R. Calderbank, "Space-time block codes from orthogonal designs," *IEEE Trans. Inf. Theory*, vol. 45, no. 5, pp. 1456-1467, Jul. 1999.

[6] A. Chockalingam and B. S. Rajan, *Large MIMO Systems*, Cambridge Univ. Press, Feb. 2014.

[7] F. Rusek, D. Persson, B. K. Lau, E. G. Larsson, T. L. Marzetta, O. Edfors, and F. Tufvesson, "Scaling up MIMO: Opportunities and challenges with very large arrays," *IEEE Signal Process. Mag.*, vol. 30, no. 1, pp. 40-60, Jan. 2013.

[8] T. L. Marzetta, "Noncooperative cellular wireless with unlimited numbers of base station antennas," *IEEE Trans. Wireless Commun.*, vol. 9, no. 11, pp. 3590-3600, Nov. 2010.

[9] A. L. Swindlehurst, E. Ayanoglu, P. Heydari, and F. Capolino, "Millimeter-wave massive MIMO: The next wireless revolution?" *IEEE Commun. Mag.*, vol. 52, no. 9, pp. 56-62, Sept. 2014

[10] E. Larsson, O. Edfors, F. Tufvesson, T. Marzetta, "Massive MIMO for next generation wireless systems," *IEEE Commun. Mag.*, vol. 52, no. 2, pp. 186-195, Feb. 2014

[11] J. Hoydis, S. ten Brink, and M. Debbah, "Massive MIMO in the UL/DL of cellular networks: How many antennas do we need?" *IEEE J. Sel. Areas Commun.*, vol. 31, no. 2, pp. 160-171, Feb. 2013.

[12] K. Zheng, L. Zhao, J. Mei, B. Shao, W. Xiang, and L. Hanzo, "Survey of large-scale MIMO systems," *IEEE Commun. Surveys Tuts.*, vol. 17, no. 3, pp. 1738-1760, Third Quart., 2015.

[13] M. Wu, B. Yu, G. Wang, *et al.*, "Large-scale MIMO detection for 3GPP LTE: algorithms and FPGA implementations," *IEEE J. Sel. Topics Signal Proc.*, vol. 8, no. 5, pp. 916-929, Oct. 2014.

[14] D. Feng, C. Jiang, G. Lim, L. J. Cimini, Jr., G. Feng, and G. Y. Li, "A survey of energy-efficient wireless communications," *IEEE Commun. Surveys Tuts.*, vol. 15, no. 1, pp. 167-178, First Quart., 2013.

[15] G. Y. Li, Z. K. Xu, C. Xiong, C. Y. Yang, S. Q. Zhang, Y. Chen, and S. G. Xu, "Energy-efficient wireless communications: Tutorial, survey, and open issues," *IEEE Wireless Commun. Mag.*, vol. 18, no. 6, pp. 28-35, Dec. 2011.

[16] R. Y. Mesleh, H. Haas, S. Sinanovic, C. W. Ahn, and S. Yun, "Spatial modulation," *IEEE Trans. Veh. Technol.*, vol. 57, no. 4, pp. 2228-2241, Jul. 2008.

[17] M. Di Renzo, H. Haas, and P. M. Grant, "Spatial modulation for multiple-antenna wireless systems: A survey," *IEEE Commun. Mag.*, vol. 49, no. 12, pp. 182-191, Dec. 2011.

[18] M. Di Renzo, H. Haas, A. Ghrayeb, S. Sugiura, and L. Hanzo, "Spatial modulation for generalized MIMO: Challenges, opportunities and implementation," *Proceedings of the IEEE*, vol. 102, no. 1, pp. 56-103, Jan. 2014.

[19] P. Yang, M. Di Renzo, Y. Xiao, S. Li, and L. Hanzo, "Design guidelines for spatial modulation," *IEEE Commun. Surveys Tuts.*, vol. 17, no. 1, pp. 6-26, First Quart., 2015.

[20] D. J. Goodman, P. S. Henry, and V. K. Prabhu, "Frequency-hopped multilevel FSK for mobile radio," *Bell Syst. Tech. J.*, vol. 59, pp. 1257-1275, Sept. 1980.

[21] T. Kawahara and T. Matsumoto, "Optimum rate reed Solomon codes for FFH/CDMA mobile radios," *IEE Elec. Letts.*, vo1. 27, no. 21, pp. 2066-2067, 1991.

[22] T. Kawahara and T. Matsumoto, "Optimal rate error protection for coded M-ary FSK FFH/CDMA mobile radio channels," *IEEE 42nd Vehicular Technology Conference (VTC)*, Denver, CO, 1992, pp. 396-399.

[23] R. Y. Mesleh, H. Haas, C. W. Ahn, and S. Yun, "Spatial modulation–A new low complexity spectral efficiency enhancing technique," *in IEEE Int. Conf. Commun. Netw. China*, Beijing, China, Oct. 2006, pp. 1-5.

[24] R. Y. Mesleh, M. Di Renzo, H. Haas, and P. M. Grant, "Trellis coded spatial modulation," *IEEE Trans. Wireless Commun.*, vol. 9, no. 7, pp. 2349-2361, Jul. 2010.

[25] R. Mesleh, H. Elgala, and H. Haas, "Optical spatial modulation," *IEEE/OSA J. Optical Commun. Netw.*, vol. 3, no. 3, pp. 234-244, Mar. 2011.

[26] Y. Yang and B. Jiao, "Information-guided channel-hopping for high data rate wireless communication," *IEEE Commun. Lett.*, vol. 12, no. 4, pp. 225-227, Apr. 2008.

[27] S. Sugiura, S. Chen, and L. Hanzo, "Generalized space-time shift keying designed for flexible diversity-, multiplexing- and complexity-tradeoffs," *IEEE Trans. Wireless Commun.*, vol. 10, no. 4, pp. 1144-1153, Apr. 2011.

[28] M. D. Renzo and H. Haas, "On transmit diversity for spatial modulation MIMO: Impact of spatial constellation diagram and shaping filters at the transmitter," *IEEE Trans. Veh. Technol.*, vol. 62, no. 6, pp. 2507-2531, Jul. 2013.

[29] M. Di Renzo and H. Haas, "Bit error probability of space shift keying MIMO over multiple-access independent fading channels," *IEEE Trans. Veh. Technol.*, vol. 60, no. 8, pp. 3694-3711, Oct. 2011.

[30] M. Di Renzo and H. Haas, "Bit error probability of SM-MIMO over generalized fading channels," *IEEE Trans. Veh. Technol.*, vol. 61, no. 3, pp. 1124-1144, Mar. 2012.

[31] M. Di Renzo and H. Haas, "Space shift keying (SSK-) MIMO over correlated Rician fading channels: Performance analysis and a new method for transmit-diversity," *IEEE Trans. Commun.*, vol. 59, no. 1, pp. 116-129, Jan. 2011.

[32] M. Di Renzo and H. Haas, "Space shift keying (SSK) modulation with partial channel state information: Optimal detector and performance analysis over fading channels," *IEEE Trans. Commun.*, vol. 58, no. 11, pp. 3196-3210, Nov. 2010.

[33] E. Başar, Ü. Aygölü, E. Panayırcı, and H. V. Poor, "New trellis code design for spatial modulation," *IEEE Trans. Wireless Commun.*, vol. 10, no. 8, pp. 2670-680, Aug. 2011.

[34] ——"Super-orthogonal trellis-coded spatial modulation," *IET Commun.*, vol. 6, no. 17, pp. 2922-2932, Nov. 2012.

[35] R. Y. Chang, S. J. Lin, and W. H. Chung, "Energy efficient transmission over space shift keying modulated MIMO channels," *IEEE Trans. Commun.*, vol. 60, no. 10, pp. 2950-2959, Oct. 2012.

[36] ——, "New space shift keying modulation with Hamming code-aided constellation design," *IEEE Wireless Commun. Lett.*, vol. 1, no. 1, pp. 2-5, Feb. 2012.

[37] J. Jeganathan, A. Ghrayeb, L. Szczecinski, and A. Ceron, "Space shift keying modulation for MIMO channels," *IEEE Trans. Wireless Commun.*, vol. 8, no. 7, pp. 3692-3703, Jul. 2009.

[38] M. Di Renzo and H. Haas, "A general framework for performance analysis of space shift keying (SSK) modulation for MISO correlated Nakagami-m fading channels," *IEEE Trans. Commun.*, vol. 58, no. 9, pp. 2590-2603, Sept. 2010.

[39] M. Di Renzo and H. Haas, "Bit error probability of space modulation over Nakagami-m fading: Asymptotic analysis," *IEEE Commun. Lett.*, vol. 15, no. 10, pp. 1026-1028, Oct. 2011

[40] M. T. Le, V. D. Ngo, H. A. Mai, X. N. Tran, and M. Di Renzo, "Spatially modulated orthogonal space-time block codes with non-vanishing determinants," *IEEE Trans. Commun.*, vol. 62, no.1, pp. 85-99, Jan. 2014.

[41] F. S. Al-Qahtani, S.Ikki, M. Di Renzo, and H. Alnuweiri, " Performance analysis of space shift keying modulation with imperfect estimation in the presence of co-channel interference," *IEEE Commun. Lett.*, vol. 18, no. 9, pp. 1587-1590, Sept. 2014.

[42] M. Di Renzo, D. De Leonardis, F. Graziosi, and H. Haas, "Space shift keying (SSK-) MIMO with practical channel estimates" *IEEE Trans. Commun.*, vol. 60, no. 4, pp. 998-1012, Apr. 2012.

[43] M. Di Renzo and H. Haas, "Improving the performance of space shift keying (SSK) modulation via opportunistic power allocation," *IEEE Commun. Lett.*, vol. 14, no. 6, pp. 500-502, Jun. 2010.

[44] F. S. Al-Qahtani, Y. Huang, M. Di Renzo, S. Ikki, and H. Alnuweiri, "Space shift keying MIMO system under spectrum sharing environments in Rayleigh fading," *IEEE Commun. Lett.*, vol. 18, no. 9, pp. 1503-1506, Sept. 2014.

[45] N. Serafimovski, S. Sinanović, M. Di Renzo, and H. Haas, " Multiple access spatial modulation," *EURASIP J. Wireless Commun. Netw.*, vol. 2012, no. 299, 2012. DOI: 10.1186/1687-1499-2012-299.

[46] A. Stavridis, S. Sinanovic, M. Di Renzo, H. Haas, and P. M. Grant, "An energy saving base station employing spatial modulation" *IEEE Int. Workshop on Computer-Aided Modeling Analysis and Design of Communication Links and Networks*, Barcelona, Spain, Sept. 2012, pp. 231-235.

[47] Y. Yang and S. Aissa, "Information-guided transmission in decode-and forward relaying systems: Spatial exploitation and throughput enhancement," *IEEE Trans. Wireless Commun.*, vol. 10, no. 7, pp. 2341-2351, Jul. 2011.

[48] R. Mesleh, S. S. Ikki, E. M. Aggoune and A. Mansour, "Performance analysis of space shift keying (SSK) modulation with multiple cooperative relays," *EURASIP Journal on Advances in Signal Processing*, Sept. 2012

[49] R. Mesleh, S. S. Ikki, and M. Alwakeel, "Performance analysis of space shift keying with amplify and forward relaying," *IEEE Commun. Lett.*, vol. 15, no. 12, pp. 1350-1352, Dec. 2011.

[50] N. Serafimovski, S. Sinanović, M. Di Renzo, and H. Haas, "Dual-hop spatial modulation (Dh-SM)," *in Proc. VTC 2011-Spring*, Budapest, Hungary, May 15-18, 2011, pp. 1-5.

[51] K. Unnikrishnan and B. Rajan, "Space-time coded spatial modulated physical layer network coding for two-way relaying," *IEEE Trans. Wireless Commun.*, vol. 14, no. 1, pp. 331-342, 2015.

[52] P. Yang, S. Li, Y. Xiao, *et al*, "Detect-and-forward relaying aided cooperative spatial modulation for wireless networks," *IEEE Trans. Commun.*,vol. 61, no. 11, pp. 4500-4511, 2013.

[53] A. Stavridis, D. Basnayaka, S. Sinanović, *et al*, "A virtual MIMO dual-hop architecture based on hybird spatial modulation," *IEEE Trans. Commun.*, vol. 62, no. 9, pp. 3161-3179, 2014.

[54] K. Ntontin, M. Di Renzo, A. I. Perez-Neira, and C. Verikoukis, "Adaptive generalized space shift keying," *EURASIP J. Wireless Commun. Netw.*, vol. 2013, no. 43, Feb. 2013.

[55] A. Younis, W. Thompson, M. Di Renzo, C.-X. Wang, M. A. Beach, H. Haas, and P. M. Grant, "Performance of spatial modulation using measured real-world channels," *IEEE Veh. Technol. Conf. - Fall*, Las Vegas, USA, 2013, pp. 1-5.

[56] N. Serafimovski, R. Mesleh, P. Chambers, M. Di Renzo, C. Wang, P. M. Grant, M. A. Beach, and H. Haas, "Practical implementation of spatial modulation," *IEEE Trans. Veh. Technol.*, vol. 62, no. 9, pp. 4511-4523, Nov. 2013.

[57] J. Zhang, Y. Wang, L. Ding, and N. Zhang, "Bit error probability of spatial modulation over measured indoor channels," *IEEE Trans. Wireless Commun.*, vol. 13, no. 3, pp. 1380-1387, Mar. 2014.

[58] A. Goldsmith, *Wireless Communications*. Cambridge, U.K.: Cambridge Univ. Press, 2005.

[59] G. L. Stuber, J. Barry, S. McLaughlin, Y. G. Li, M. A. Ingram, and T. Pratt, "Broadband MIMO-OFDM wireless communications," *Proceedings of the IEEE*, vol. 92, no. 2, pp. 271-294, Feb. 2004.

[60] M. I. Kadir, S. Sugiura, S. Cheng, and L. Hanzo, "Unified MIMO-multicarrier designs: A space-time shift keying approach," *IEEE Commun. Surveys Tuts.*, vol. 17, no. 2, pp. 550-579, 2015.

[61] B. Muquet, Z. Wang, G. Giannakis, M. de Courville, and P. Duhamel, "Cyclic prefixing or zero padding for wireless multicarrier transmissions?" *IEEE Trans. Commun.*, vol. 50, no. 12, pp. 2136-2148, Dec. 2002.

[62] N. Benvenuto, R. Dinis, D. Falconer, and S. Tomasin, "Single carrier modulation with nonlinear frequency domain equaliza-

tion: An idea whose time has come–again," *Proceedings of the IEEE*, vol. 98, no. 1, pp. 69-96, Jan. 2010.

[63] A. Pitarokoilis, S. K. Mohammed, and E. G. Larsson, "On the optimality of single-carrier transmission in large-scale antenna systems," *IEEE Wireless Commun. Lett.*, vol. 1, no. 4, Apr. 2012.

[64] L. Lu, G. Y. Li, A. L. Swindlehurst, A. Ashikhmin, and R. Zhang, "An overview of massive MIMO: Benefits and challenges," *IEEE J. Sel. Topics Signal Proc.*, vol. 8, no. 5, pp. 742-758, Oct. 2014.

[65] Y. Sheng, Z. Tan, and G. Y. Li, "Single-carrier modulation with ML equalization for large-scale antenna systems over Rician Fading channels," *IEEE International conference on acoustic, speech and signal processing (ICASSP)*, Florence, 2014, pp. 5759 - 5763.

[66] B. Zhou, Y. Xiao, P. Yang, J. Wang, and S. Li, "Spatial modulation for single carrier wireless transmission systems," *2011 6th International ICST Conference on Communications and Networking in China*, Harbin, Aug. 2011, pp. 11-15.

[67] N. Serafimovski, M. Di Renzo, S. Sinanović, R. Y. Mesleh, and H. Haas, "Fractional bit encoded spatial modulation (FBE-SM)," *IEEE Commun. Lett.*, vol. 14, no. 5, pp. 429-431, May 2010.

[68] Y. Yang and S. Aissa, "Bit-padding information guided channel hopping," *IEEE Commun. Lett.*, vol. 15, no. 2, pp. 163-165, Feb. 2011.

[69] A. G. Orozco-Lugo, M. M. Lara, and D. C. McLernon, "Channel estimation using implicit training," *IEEE Transs. Signal Process.*, vol. 52, no. 1, pp. 240-254, Jan. 2004.

[70] P. Som and A. Chockalingam, "Spatial modulation and space shift keying in single carrier communication," *in 2012 IEEE 23rd International Symposium on PIMRC*, Sydney, Sept. 2012, pp. 1991-1996.

[71] R. Rajashekar, K.V.S. Hari, and L. Hanzo, "Spatial modulation aided zero-padded single carrier transmission for dispersive channels," *IEEE Trans. Commun.*, vol. 61, no. 6, pp. 2318-2329, Jun. 2013.

[72] S. M. Alamouti, "A simple transmit diversity technique for wireless communications," *IEEE J. Sel. Areas Commun.*, vol. 16, no. 8, pp. 1451-1458, Oct. 1998.

[73] J. Fu, C. Hou, W. Xiang, L. Yan, and Y. Hou, "Generalised spatial modulation with multiple active transmit antennas," *Proc. IEEE GLOBECOM 2010 Workshops*, pp. 839-844, Dec. 2010.

[74] T. Datta and A. Chockalingam, "On generalized spatial modulation," *Proc. IEEE WCNC 2013*, Apr. 2013.

[75] J. Wang, S. Jia, and J. Song, "Generalised spatial modulation system with multiple active transmit antennas and low complexity detection scheme," *IEEE Trans. Wireless Commun.*, vol. 11, no. 4, pp. 1605-1615, Apr. 2012.

[76] J. Jeganathan, A. Ghrayeb, and L. Szczecinski, "Generalized space shift keying modulation for MIMO channels," *in Proc. IEEE Int. Symp. Pers., Indoor, Mobile Radio Commun.*, Cannes, France, Sep. 2008, pp. 1-5.

[77] S. Sugiura, S. Chen, and L. Hanzo, "Coherent and differential space time shift keying: A dispersion matrix approach," *IEEE Trans. Commun.*, vol. 58, no. 11, pp. 3219-3230, Nov. 2010.

[78] T. L. Narasimhan, P. Raviteja, and A. Chockalingam, "Generalized spatial modulation in large-scale multiuser MIMO systems," *IEEE Trans. Wireless Commun.*, vol. 24, no. 7, pp. 3764-3779, 2015.

[79] J. Zheng and Y. Sun, "Energy-efficient spatial modulation over MIMO frequency selective fading channels," *IEEE Trans. Veh. Technol*, vol. 64, no. 5, pp. 2204-2209, 2015.

[80] H. A. Ngo, C. Xu, S. Sugiura, and L. Hanzo, "Space-time-frequency shift keying for dispersive channels," *IEEE Signal Process. Lett.*, vol. 18, no. 3, pp. 177-180, Mar. 2011.

[81] A. Younis, N. Serafimovski, R. Mesleh, and H. Haas, "Generalised spatial modulation," *in Proc. Signals, Syst. Comput.*, Pacific Grove, CA, Nov. 2010, pp. 1498-1502.

[82] J. G. Proakis, *Digital Communications*, 4th ed. New York, NY, USA: McGraw-Hill, 2004.

[83] R. W. Heath, Jr. and A. J. Paulraj, "Linear dispersion codes for MIMO systems based on frame theory," *IEEE Trans. Signal Process.*, vol. 50, no. 10, pp. 2429-2441, Oct. 2002.

[84] J. Jeganathan, A. Ghrayeb, and L. Szczecinski, "Spatial modulation: Optimal detection and performance analysis," *IEEE Commun. Lett.*, vol. 12, no. 8, pp. 545-547, Aug. 2008.

[85] S. Sugiura, C. Xu, S. X. Ng, and L. Hanzo, "Reduced-complexity coherent versus non-coherent QAM-aided space-time shift keying," *IEEE Trans. Commun.*, vol. 59, no. 11, pp. 3090-3101, Nov. 2011.

[86] S. Sugiura, S. Chen, and L. Hanzo, "MIMO-aided near-capacity turbo transceivers: Taxonomy and performance versus complexity," *IEEE Commun. Surveys Tuts.*, vol. 14, no. 2, pp. 421-442, Second Quart. 2012.

[87] S. Sugiura and L. Hanzo, "Single-RF spatial modulation requires single-carrier transmission: frequency-domain turbo equalization for dispersive channels," *IEEE Trans. Veh. Technol.*, vol. 64, no. 10, pp. 4870-4875, 2015.

[88] L. Xiao, D. Lilin, Y. Zhang, Y. Xiao, P. Yang, and S. Li, "A low-complexity detection scheme for generalized spatial modulation aided single carrier systems," *IEEE Commun. Lett.*, vol. 19, no. 6, pp. 1069-1072, 2015.

[89] J. Zhang, L. Yang, and L. Hanzo, "Advances in cooperative single-carrier FDMA communications: Beyond LTE-Advanced," *IEEE Commun. Surveys Tuts.*, vol. 17, no. 2, pp. 730-756, 2015.

[90] F. Pancaldi, G. Vitetta, R. Kalbasi, N. Al-Dhahir, M. Uysal, and H. Mheidat, "Single-carrier frequency domain equalization," *IEEE Signal Process. Mag.*, vol. 25, no. 5, pp. 37-56, Sept. 2008.

[91] A. H. Mehana and A. Nosratinia, "Diversity of MMSE MIMO receivers," *IEEE Trans. Inf. Theory*, vol. 51, no. 11, pp. 6788-6805, Nov. 2012.

[92] O. D. Mohamed, El Hesham, and G. Caire, "On maximum-likelihood detection and the search for the closest lattice point," *IEEE Trans. Inf. Theory*, vol. 47, no. 10, pp. 2389-2402, 2003.

[93] A. Younis, S. Sinanovic, M. Di Renzo, R. Y. Mesleh, and H. Haas, "Generalised sphere decoding for spatial modulation," *IEEE Trans. Commun*, vol. 61, no. 7, pp. 2805-2815, Jul. 2013.

[94] L. Hanzo, T. H. Liew, B. L. Yeap, R. Y. S. Tee and S. X. Ng, *Turbo Coding, Turbo Equalisation, and Space-Time Coding: EXIT-Chart-aided Near-Capacity Designs for Wireless Channels, 2nd Edition.* Hoboken, NJ, USA: Wiley, 2011.

[95] E. Candes, J. Romberg, and T. Tao, "Robust uncertainty principles: Exact signal reconstruction from highly incomplete frequency information," *IEEE Trans. Inf. Theory*, vol. 52, no. 2, pp. 489-509, Feb. 2006.

[96] D. Donoho, "Compressed sensing," *IEEE Trans. Inf. Theory*, vol. 52, no. 4, pp. 1289-1306, 2006.

[97] A. Stavridis, S. Sinanovic, M. Di Renzo, and H. Haas, "Energy evaluation of spatial modulation at a multi-antenna base station," *in Proc. IEEE Veh. Technol. Conf.-Fall*, Barcelona, Spain, Sept. 2013, pp. 1-5.

[98] E. Başar, Ü. Aygölü, E. Panayırcı, and H. V. Poor, "Space-time block coded spatial modulation," *IEEE Trans. Commun.*, vol. 59, no. 3, pp. 823-832, Mar. 2011.

[99] 3GPP TR36.814, *Evolved Universal Terrestrial Radio Access (E-UTRA): Further Advancements for E-UTRA Physical Layer Aspects*, v. 9.0.0, Mar. 2010.

[100] S. Narayanan, M. J. Chaudhry, A. Stavridis, M. Di Renzo, F. Graziosi, and H. Haas, "Multi-user spatial modulation MIMO," *in Proc. IEEE WCNC 2014*, Istanbul, Apr. 2014, pp. 671-676.

[101] K. M. Humadi, A. I. Sulyman, and A. Alsanie, "Spatial modulation concept for massive multiuser MIMO systems," *International Journal of Antenna and Propagation*, vol. 2014, 1-9, 2014.

[102] R. Zhang, L. Yang, and L. Hanzo, "Generalised pre-coding aided spatial modulation," *IEEE Trans. Wireless Commun.*, vol. 12, no. 11, pp. 5434-5443, 2013.

[103] R. Zhang, L.-L. Yang, and L. Hanzo, "Error probability and capacity analysis of generalized pre-coding aided spatial modulation," *IEEE Trans. Wireless Commun.*, vol. 14, no. 1, pp. 364-375, Jan. 2015.

[104] A. Stavridis, D. Basnayaka, S. Sinanovic, M. Di Renzo, and H. Haas, "A virtual MIMO dual-hop architecture based on hybrid spatial modulation," *IEEE Trans. Commun.*, vol. 62, no. 9, pp. 3161-3179, Sep. 2014.

[105] T. L. Narasimhan P. Raviteja, and A. Chockalingam, "Large-scale multiuser SM-MIMO versus massive MIMO," *in Inform. Theory and Applications Workshop (ITA)*, Feb. 2014, pp. 56-62.

[106] J. Zheng, "Low-complexity detector for spatial modulation multiple access channels with a large number of receive antennas," *IEEE Commun. Letters*, vol. 18, no. 11, pp. 2055-2058, Nov 2014.

[107] A. Garcia Rodriguez, C. Masouros, "Low-complexity compressive sensing detection for spatial modulation in large-scale multiple access channels," *IEEE Trans. Commun.*, vol. 63, no. 7, pp. 2565-2579, 2015.

[108] B. J. Frey, *Graphical Models for Machine Learning and Digital Communication*, Cambridge: MIT Press, 1998.

[109] R. J. McEliece, D. J. C. MacKay, and J-F. Cheng, "Turbo decoding as an instance of Pearls "belief propagation" algorithm," *IEEE J. Sel. Areas Commun.*, vol. 16, no. 2, pp. 140-152, Feb. 1998.

[110] T. L. Narasimhan and A. Chockalingam, "Channel hardening-exploiting message passing (CHEMP) receiver in large-scale MIMO systems," *IEEE J. Sel. Topics in Signal Process.*, vol. 8, no. 5, pp. 847-860, Oct. 2014.

[111] B. J. Frey and D. Dueck, "Clustering by passing messages between data points," *Science*, vol. 315, pp. 972-976, Feb. 16, 2007.

[112] S. Wang, Y. Li, M. Zhao and J. Wang, "Energy efficient and low-complexity uplink transceiver for massive spatial modulation MIMO," *IEEE Trans. Veh. Technol.*, vol. 64, no. 10, pp. 4617-4632, 2015.

[113] S. Wang, Y. Li, and J. Wang, "Multiuser detection in massive spatial modulation MIMO with low-resolution ADCs," *IEEE Trans. Wireless Commun.*, vol. 14, no. 4, pp. 2156-2168, 2015.

[114] C. M. Yu, S. H. Hsieh, H. W. Liang, C. S. Lu, W. H. Chung, S. Y. Kuo, and P. S. Chang, "Compressed sensing detector design for space shift keying in MIMO systems," *IEEE Commun. Lett.*, vol. 16, no. 10, pp. 1556-1559, Oct. 2012.

[115] W. Liu, N. Wang, M, J, and H. Xu, "Denoising detection for the generalized spatial modulation system using sparse property," *IEEE Commun. Lett.*, vol. 18, no. 1, pp. 22-25, Jan. 2014.

[116] X. Peng, W. Wu J. Sun, and Y. Liu, "Sparse K-best detector for generalised space shift keying in large-scale multiple-input-multiple-output systems," *IET Communications*, vol. 9, no. 6, pp. 771-778, 2015.

[117] K. Ishibashi and S. Sugiura, "Effects of antenna switching on band-limited spatial modulation," *IEEE Wireless Commun. Lett.*, vol. 3, no. 4, pp. 345-348, Apr. 2014.

[118] M. S. Sedaghat, R. R. Mueller, and G. Fischer, "A novel single-RF transmitter for massive MIMO," *Smart Antennas (WSA), 2014 18th International ITG Workshop on*, Erlangen, Germany, March 2014, pp. 1-8.

[119] L. Hanzo, S. X. Ng, T. Keller, and W. Webb, *Quadrature Amplitude Modulation: From Basics to Adaptive Trellis-Coded, Turbo-Equalised and Space-Time Coded OFDM, CDMA and MC-CDMA Systems*. John Wiley and IEEE Press, 2004.

[120] K. V. Vardhan, S. K. Mohammed, A. Chockalingam, and B. S. Rajan, "A low-complexity detector for large MIMO systems and multicarrier CDMA systems," *IEEE J. Sel. Areas Commun.*, vol. 26, no. 3, pp. 473-485, Apr. 2008.

[121] S. K. Mohammed, A. Zaki, A. Chockalingam, and B. S. Rajan, "High rate space time coded large-MIMO systems: low-complexity detection and channel estimation," *IEEE J. Sel. Topics Signal Proc.*, vol. 3, no. 6, pp. 958-974, Dec. 2009.

[122] N. Srinidhi, T. Datta, A. Chockalingam, and B. S. Rajan, "Layered tabu search algorithm for large-MIMO detection and a lower bound on ML performance," *IEEE Trans. Commun.*, vol. 59, no. 11, pp. 2955-2963, Nov. 2011.

[123] T. Datta, N. A. Kumar, A. Chockalingam, and B. S. Rajan, "A novel Monte Carlo sampling based receiver for large-scale uplink multiuser MIMO systems," *IEEE Trans. Veh. Technol.*, vol. 62, no. 7, pp. 3019-3038, Sept. 2013.

[124] P. Raviteja, T. L. Narasimhan, and A. Chockalingam, "Detection in large scale multiuser SM-MIMO systems: algorithms and performance," *in Proc. IEEE VTC 2014-Spring*, May 2014.

[125] S. Sanayei and A. Nosratinia, "Antenna selection in MIMO systems," *IEEE Commun. Mag.*, vol. 42, no. 10, pp. 68-73, Oct. 2004.

[126] P. Zhang, S. Chen, C. Dong, L. Li, and L. Hanzo, "Two-tier channel estimation aided near-capacity MIMO transceivers relying on norm-based joint transmit and receive antenna selection," *IEEE Trans. Wireless Commun.*, vol. 14, no. 1, pp. 122-137, 2015.

[127] Z. Zhou, N. Ge, and X. Lin, "Reduced-complexity antenna selection schemes in spatial modulation," *IEEE Commun. Lett.*, vol. 18, no. 1, pp. 14-17, Jun. 2014.

[128] R. Rajashekar, K. V. S. Hari, and L. Hanzo, "Antenna selection in spatial modulation systems," *IEEE Commun. Lett.*, vol. 17, no. 3, pp. 521-524, Mar. 2013.

[129] K Ntontin, M. Di Renzo, A. Perez-Neira, and C. Verikoukis, "A low-complexity method for antenna selection in spatial modulation systems," *IEEE Commun. Lett.*, vol. 17, no. 12, pp. 2312-2315, Aug. 2013.

[130] N. Wang, W. Liu, H. Men, M. Jin, and H. Xu. "Further complexity reduction using rotational symmetry for EDAS in spatial modulation," *IEEE Commun. Lett.*, vol. 18, no. 10, pp. 1835-1838, 2014.

[131] J. Zheng, "Fast receive antenna subset selection for pre-coding aided spatial modulation," *IEEE Wireless Commun. Lett.*, vol. 4, no. 3, pp. 317-320, 2015.

[132] J. Zheng and J. Chen, "Further complexity reduction for antenna selection in spatial modulation systems," *IEEE Commun. Lett.*, vol. 19, no. 6, pp. 937-940, 2015.

[133] A. Mohammadi and F. M. Ghannouchi, "Single RF front-end MIMO transceivers," *IEEE Commun. Mag.*, vol. 49, no. 12, pp. 104-109, Dec. 2011.

[134] P. Banelli *et al.*, "Modulation formats and waveforms for 5G networks: Who will be the heir of OFDM?: An overview of alternative modulation schemes for improved spectral efficiency," *IEEE Signal Process. Mag.*, vol. 31, no. 6, pp. 80-93, Nov. 2014.

[135] D. J. Love, R. W. Heath, V. K. N. Lau, D. Gesbert, B. D. Rao, and M. Andrews, "An overview of limited feedback in wireless communication systems," *IEEE J. Sel. Areas Commun.*, vol. 26, no. 8, pp. 1341-1365, Oct. 2008.

[136] C. B. Chae, A. Forenza, R. W. Heath, Jr., M. R. Mckay, and I. B. Collings, "Adaptive MIMO transmission techniques for broadband wireless communication systems," *IEEE Commun. Mag.*, vol. 48, no. 5, pp. 112-118, May 2010.

[137] P. Yang, Y. Xiao, Y. Yi, and S. Li, "Adaptive spatial modulation for wireless MIMO transmission systems," *IEEE Commun. Lett.*, vol. 15, no. 6, pp. 602-604, Jun. 2011.

[138] P. Yang, Y. Xiao, L. Li, Q. Tang, Y. Yu, and S. Li, "Link adaptation for spatial modulation with limited feedback," *IEEE Trans. Veh. Technol.*, vol. 61, no. 8, pp. 3808-3813, Oct. 2012.

[139] M. Maleki, H. R. Bahrami, S. Beygi, M. Kafashan, and N. H. Tran, "Space modulation with CSI: Constellation design and performance evaluation," *IEEE Trans. Veh. Technol.*, vol. 62, no. 4, pp. 1623-1634, May 2013.

[140] M. Maleki, H. R. Bahrami, M. Kafashan, and N. H. Tran, "On the performance of spatial modulation: optimal constellation breakdown," *IEEE Trans. Commun.*, vol. 62, no. 1, pp. 144-157,Jan. 2014.

[141] C. Masouros and L. Hanzo, "Constellation-randomization achieves transmit diversity for single-RF spatial modulation," *IEEE Trans. Veh. Tech.*, in press, 2015. http://discovery.ucl.ac.uk/1462459/1/Masouros_SM-Const Rand5.pdf.

[142] A. Garcia, C. Masouros and L. Hanzo, "Pre-scaling optimization for space shift keying based on semidefinite relaxation" *IEEE Trans. Commun.*, vol. 63, no. 11, pp. 4231-4243, 2015.

[143] P. Yang, Y. Xiao, B. Zhang, S. Li, M. El-Hajjar, and L. Hanzo, "Power allocation aided spatial modulation for limited-feedback MIMO systems," *IEEE Trans. Veh. Technol.*, vol. 64, no. 5, pp. 2198-2204, 2015.

[144] P. Yang, Y. Xiao, S. Li, and L. Hanzo, "A low-complexity power allocation algorithm for multiple-input multiple-output spatial modulation systems," *IEEE Trans. Veh. Technol.*, 2015, in press, DOI: 10.1109/TVT.2015.2410252.

[145] D. Yang, C. Xu, L.-L. Yang, and L. Hanzo, "Transmit-diversity-assisted space-shift keying for colocated and distributed/cooperative MIMO elements," *IEEE Trans. Veh. Technol.*, vol. 60, no. 6, pp. 2864-2869, Jul. 2011.

[146] C. Masouros, "Improving the diversity of spatial modulation in MISO channels by phase alignment," *IEEE Commun. Lett.*, vol. 18, no. 5, pp. 729-732, 2014.

[147] P. Yang, Y. Xiao, S. Li, and L. Hanzo, "Phase rotation-based precoding for spatial modulation systems," *IET Communications*, vol. 9, no. 10, pp. 1315-1323, 2015.

[148] M. S. Veedu, C. R. Murthy, L. Hanzo, "Single-RF spatial modulation relying on finite-rate phase-only feedback: Design and analysis," *IEEE Trans. Veh. Technol.*, 2015, in press, DOI:10.1109/TVT.2015.2424960.

[149] P. Yang, Y. L. Guan, Y. Xiao, M. Di. Renzo and S. Li, "Transmit pre-coding aided spatial modulation maximum the minimum Euclidean distance versus minimum the BER," *IEEE Trans. Wireless Commun.*, 2015, in press, DOI:10.1109/TWC.2015.2497692.

[150] H. Li, L. Song, D. Zhu, and M. Lei, "Energy efficiency of large scale MIMO systems with transmit antenna selection," *in Proc. IEEE Int. Conf. Commun. (ICC)*, Jun. 2013.

[151] R. Kudo, S. M. D. Armour, J. P. McGeehan, and M. Mizoguchi, "A channel state information feedback method for massive MIMO OFDM," *IEEE J. Commun. and Netw.*, vol. 15, no. 4, pp. 352-361, Aug. 2013.

[152] E. Başar, Ü. Aygölü, E. Panayırcı, and H. V. Poor, "Performance of spatial modulation in the presence of channel estimation errors," *IEEE Commun. Lett.*, vol. 16, no. 2, pp. 176-179, Feb. 2012.

[153] S. S. Ikki and R. Mesleh, "A general framework for performance analysis of space shift keying (SSK) modulation in the presence of Gaussian imperfect estimations," *IEEE Commun. Lett.*, vol. 16, no. 2, pp. 228-230, Feb. 2012.

[154] S. Sugiura and L. Hanzo, "Effects of channel estimation on spatial modulation," *IEEE Signal Process. Lett.*, vol. 19, no. 12, pp. 805-808, Dec. 2012.

[155] X. Wu, H. Claussen, M. Di Renzo, and H. Haas, "Channel estimation for spatial modulation," *IEEE Trans. Commun.*, vol. 62, no. 12, pp.4362-4372, Dec. 2014.

[156] Z. Liu, U. Parampalli, and Y. L. Guan, "Optimal odd-length binary Z-complementary pairs," *IEEE Trans. Inf. Theory*, vol. 60, no. 9, pp. 5768-5781, Jul. 2014.

[157] Z. Liu, Y. Li, and Y. L. Guan, "New constructions of general QAM Golay complementary sequences,"*IEEE Trans. Inf. Theory*, vol. 59, no. 11, pp. 7684-7692, Nov. 2013.

[158] Z. Liu, Y. L. Guan and U. Parampalli, "New complete complementary codes for the peak-to-mean power control in MC-CDMA," *IEEE Trans. Commun.*, vol. 62, no. 3, pp. 1105-1113, Mar. 2014

[159] Z. Liu, Y. L. Guan and H. H. Chen, "Fractional-delay-resilient receiver for interference-free MC-CDMA communications based on complete complementary codes" *IEEE Trans. Wireless Commun.*, vol. 14, no. 3, pp. 1226-1236, Oct. 2014.

[160] M. El-Fandi, I. A. Henderson, J. McGhee, and P. McGlone, "Uncorrelated multisymbol signals for MIMO system identification," *IEEE Trans. Instrum. Meas.*, vol. 47, no. 10, pp. 1133-1138, Oct. 1998.

[161] S. Chen, S. Sugiura, and L. Hanzo, "Semi-blind joint channel estimation and data detection for space-time shift keying systems," *IEEE Signal Process. Lett.*, vol. 17, no. 12, pp. 993-996, Dec. 2010.

[162] R. Rajashekar, K.V.S. Hari, and L. Hanzo, "Reduced complexity ML detection and capacity-optimized training for spatial modulation systems," *IEEE Trans. Commun.*, vol. 62, no. 1, pp. 112-125, Jan. 2014.

[163] M. Wen, Z. Ding, X. Cheng, Y. Bian, H. V. Poor, and B. Jiao, "Performance analysis of differential spatial modulation with two transmit antennas," *IEEE Commun. Lett.*, vol. 18, no. 3, pp. 475-478, Mar. 2014.

[164] N. Ishikawa and S. Sugiura, "Unified differential spatial modulation," *IEEE Wireless Commun. Lett.*, vol. 3, no. 4, pp. 337-340, Feb. 2014.

[165] Y. Bian, X. Cheng, M. Wen, L. Yang, H. V. Poor, and B. Jiao, "Differential spatial modulation," *IEEE Trans. Veh. Technol.*, vol. 64, no. 7, pp. 3262-3268, 2015.

[166] M. Wen, X. Cheng, Y. Bian, and H.V. Poor, "A low-complexity near-ML differential spatial modulation detector," *IEEE Signal Process. Lett.*, vol. 22, no. 11, pp.1834-1838, Nov. 2015.

[167] P. A. Martin, "Differential spatial modulation for APSK in time-varying fading channels," *IEEE Commun. Lett.*, vol. 19, no. 7, pp. 1261-1264, Jul. 2015.

[168] L. Xiao, P. Yang, X. Lei, Y. Xiao, and S. Li, "A low-complexity detection scheme for differential spatial modulation," *IEEE Commun. Lett.*, vol. 19, no. 9, pp. 1516-1519, 2015.